British Journal of Cancer (2005) 92, 1877–1880

www.bjcancer.com

Gefitinib treatment affects androgen levels in non-small-cell lung cancer patients

M Nishio*[,1], F Ohyanagi[1], A Horiike[1], Y Ishikawa[3], Y Satoh[2], S Okumura[2], K Nakagawa[2], K Nishio[4] and T Horai[1]

[1]Division of Internal Medicine, Cancer Institute Hospital, Japanese Foundation For Cancer Research, Ariake 3-10-6, Koto-ku, Tokyo 135-8550, Japan; [2]Department of Chest Surgery, Cancer Institute Hospital, Japanese Foundation For Cancer Research, Tokyo, Japan; [3]Department of Pathology, Cancer Institute, Japanese Foundation For Cancer Research, Tokyo, Japan; [4]Pharmacology Division, National Cancer Center Research Institute, Tokyo, Japan

Gefitinib, an inhibitor of the epidermal growth factor receptor (EGFR, HER1/ErbB1) tyrosine kinase, has been shown to have clinical activity against non-small-cell lung cancers (NSCLCs), especially in women nonsmokers with adenocarcinomas. The aim of the present study was to clarify the relationship between androgen levels and gefitinib treatment in patients with advanced NSCLCs. Sera from 67 cases (36 men and 31 women) were obtained pretreatment and during treatment with gefitinib monotherapy (days 14–18) for examination of testosterone, dehydroepiandrosterone sulphate (DHEA), and dehydroepiandrosterone sulphate (DHEAS) levels. Testosterone and DHEA during treatment were significantly lower than the pretreatment values in both women and men, and the DHEAS levels during treatment were also significantly lowered in women. Gefitinib treatment significantly suppressed androgen levels, especially in women who had no smoking history. In addition, hormone levels in women responding to gefitinib were significantly lower during the treatment than in women who did not respond. Gefitinib-associated decrease in serum androgen levels may play a role in its clinical efficacy.

British Journal of Cancer (2005) **92,** 1877–1880. doi:10.1038/sj.bjc.6602585 www.bjcancer.com
Published online 3 May 2005

Keywords: sex hormone; epidermal growth factor receptor; tyrosine kinase inhibitor

Non-small-cell lung cancer (NSCLC) is a major health problem worldwide for both men and women (Ferlay *et al*, 2001). Usually at the time of diagnosis more than 50% of the patients have advanced or metastatic disease. While cytotoxic chemotherapy slightly prolongs survival among advanced NSCLC patients, it exerts clinically significant adverse effects (Non-Small-Cell Lung Cancer Collaborative Group, 1995; Schiller *et al*, 2002). An effective, palliative, low-toxicity treatment for patients with advanced NSCLC is therefore needed and for this purpose the epidermal growth factor receptor (EGFR/HER1) is a promising target. Gefitinib (ZD 1839, Iressa; AstraZeneca, London, UK) is an orally active, selective HER1-tyrosine kinase inhibitor (Wakeling *et al*, 2002), which has been shown to elicit objective responses in NSCLC cases, particularly in women nonsmokers with adenocarcinomas (Fukuoka *et al*, 2003; Kris *et al*, 2003). Recently, active mutations of EGFR have been identified in such cases (Paez *et al*, 2004; Pao *et al*, 2004) and may be linked with the sensitivity to gefitinib (Lynch *et al*, 2004; Paez *et al*, 2004; Pao *et al*, 2004). However, the reason why mutations frequently occur in these particular individuals is poorly understood.

Androgens are important hormones that play definitive roles in the differentiation of males and females. They can modify the activity of the epidermal growth factor network and EGFR signaling is essential for androgen-induced proliferation (Klein and Nielsen, 1993; Dammann *et al*, 2000; Torring *et al*, 2003). A receptor for androgens has been reported to occur in NSCLCs (Beattie *et al*, 1985; Kaiser *et al*, 1996) and there may be cooperative interaction between the hormones and active mutations of EGFR during the development of lung cancer. Previous reports have suggested that smoking increases the levels of androgens in men and women (Law *et al*, 1997; Trummer *et al*, 2002) and carcinogens from cigarette smoke may disrupt androgen function by reducing androgen receptor (AR) levels in androgen-responsive organs (Lin *et al*, 2004).

On the basis of these reports, we hypothesised that androgens may play an important role in the efficacy of gefitinib in NSCLC cases. In the present study, we therefore evaluated androgen levels in patients treated with gefitinib and the relationship with clinical efficacy.

PATIENTS AND METHODS

Between September 2002 and May 2004, 67 advanced or recurrent NSCLC patients were analysed in this study. All 67 were treated at our institution with gefitinib monotherapy (250 mg oral doses of gefitinib once daily) until disease progression occurred. Response evaluation and confirmation were performed in accordance with the WHO criteria (WHO, 1979). In brief, complete response (CR) was defined as complete disappearance of all lesions in imaging studies for at least 4 weeks without the appearance of any new lesions. Partial response (PR) was defined as a >50% decrease under the baseline in the sum of the products of the

*Correspondence: Dr M Nishio; E-mail: mnishio@jfcr.or.jp
Received 13 December 2004; revised 21 March 2005; accepted 21 March 2005; published online 3 May 2005

perpendicular diameters of all measurable lesions and at least stabilisation of all nonmeasurable lesions over a minimum period of 4 weeks. Progressive disease (PD) was defined as a >25% increase in the sum of the products of all measurable lesions, an unequivocal increase of nonmeasurable disease, or the appearance of new lesions. Cases were classified as having stable disease (SD) if none of the criteria for classifying responses as a CR, PR, or PD were met.

Blood was drawn before and during gefitinib administration. A previous report indicated the median time to symptom improvement with gefitinib to be only 8 days (Fukuoka *et al*, 2003), and we therefore checked the hormone levels at days 14–18, when serum was sampled between 10:00 and 14:00 and stored at 80°C for subsequent analyses. Serum levels of testosterone, dehydroepiandrosterone (DHEA), and dehydroepiandrosterone sulphate (DHEAS) were all measured at the SRL Laboratory (Tokyo, Japan). For testosterone, an electrochemiluminescence immunoassay was applied (ECLusys testosterone; Roche Diagnostics KK, Tokyo, Japan) and radioimmunoassays were used for DHEA and DHEAS (DPC DHEA and DPC DHEAS kits; Diagnostic Products Corporation, Los Angeles, CA, USA). The detection limits for testosterone, DHEA, and DHEAS were 5, 0.2, and 20 ng ml^{-1}, respectively. Inter- and intra-assay coefficients of variation were 6 and 8% for testosterone, 8 and 9% for DHEA, and 4 and 4% for DHEAS, respectively.

Appropriate ethical review boards approved the study, which followed the recommendations of the Declaration of Helsinki for biomedical research involving human subjects.

Statistical analysis

A paired *t*-test was used to compare the androgen levels between the two time periods. Patients were grouped into responders (CR and PR) and nonresponders (SD and PD) and the variables in each group were compared with an unpaired *t*-test. All statistical analyses were performed using SPSS version 8 statistical software (SPSS Inc., IL, USA).

RESULTS

Patient characterisation

Data for patient characteristics are listed in Table 1. Of the 67, 31 (46.3%) were women. The median age was 61 years (range, 42–80 years). There were 26 patients (38.8%) who had never smoked and adenocarcinoma was the primary histological finding in 56 cases (83.6%). There was no prior chemotherapy in 16 (23.9%) of the patients, and the remainder had received platinum-based chemotherapy.

Response to treatment could only be evaluated in 64 of the 67 cases. We observed 20 PR (29.8%), and of these, 13 (65%) were women and seven (35%) were men ($P=0.074$). The median and range of treatment duration with gefitinib were 2.1 and 0.2–21 months. In all, 10 (50%) of 20 responders and 29 (66%) of 44 nonresponders had a smoking history ($P=0.226$).

Effects of gefitinib treatment on androgens levels in NSCLC patients

Testosterone, DHEA, and DHEAS were detected in the serum of all 67 patients (see Table 2). There was a significant difference observed between men and women for serum testosterone levels ($P<0.0001$), but not for serum DHEA or DHEAS (DHEA; $P=0.267$, DHEAS; $P=0.0565$).

In women, testosterone, DHEA, and DHEAS levels at pretreatment were significantly higher than during treatment (testosterone; $P=0.025$, DHEA; $P=0.0065$, DHEAS; $P=0.0326$). In men, pretreatment testosterone and DHEA levels were significantly higher than during treatment, but there was no significant difference for DHEAS (testosterone, $P=0.0009$; DHEA, $P=0.0085$; DHEAS, $P=0.33$). In addition, we compared hormone levels between smokers and nonsmokers. Pretreatment, there were no significant differences between women with and without a smoking history. On the other hand, hormone levels were significantly suppressed by gefitinib treatment in the 21 women who had no smoking history (testosterone, $P=0.0016$; DHEA,

Table 1 Patient characteristics

Variable	No. of patients	%
Total	67	
Sex		
Male	36	53.7
Female	31	46.3
Age (years)		
Median	61	
Range	42–80	
Smoking history		
Never	26	38.8
Former/current	41	61.2
Performance status		
0, 1	48	71.6
>2	19	28.4
Histology		
Ad	56	83.6
Non-Ad	11	16.4
Stage		
II–III	17	25.4
IV	27	40.3
Recurrence after surgery	23	34.3
Response		
PR	20	29.8
SD/PD	44	64.7
NE	3	4.5
Prior chemotherapy		
No	16	23.9
Yes	51	76.1

Ad = adenocarcinoma; non-Ad = nonadenocarcinoma; PR = partial response; SD = stable disease; PD = progressive disease; NE = not evaluable.

Table 2 Androgen levels in patients treated with gefitinib

	Pretreatment		During treatment		
Variable	***n***	**Mean±s.d.**	***n***	**Mean±s.d.**	**Paired *t*-test**
Testosterone (ng ml^{-1})					
Female		21.5±12.0	31	13.8.0±11.0	$P=0.025$
Male	37	409.7±129.8	37	350.8±135.7	$P=0.0009$
DHEA (ng ml^{-1})					
Female	31	2.21±2.03	31	1.33±0.83	$P=0.0065$
Male	37	1.78±1.06	37	1.49±0.92	$P=0.0085$
DHEAS (ng ml^{-1})					
Female	31	854.4±579.5	31	645.8±365.6	$P=0.0326$
Male	37	1137.4±607.7	37	1103.0±601.5	$P=0.33$

s.d. = standard deviation; DHEA = dehydroepiandrosterone; DHEAS = dehydroepiandrosterone sulphate.

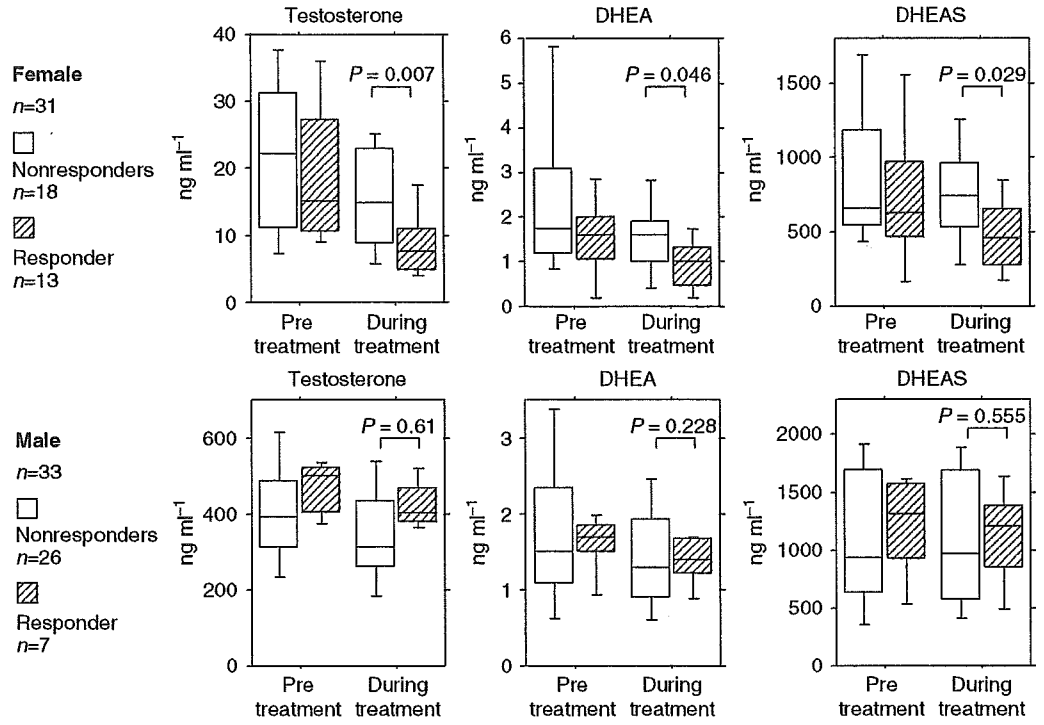

Figure 1 Serum testosterone, DHEA, and DHEAS levels, pretreatment and during the gefitinib administration. Each androgen levels are depicted in accordance to clinical response of gefitinib treatment (responders, PR; nonresponders, SD or PD). Error bars showed standard deviation.

$P=0.0157$; DHEAS, $P=0.0441$), but not in the 10 who had a smoking history (testosterone, $P=0.6159$; DHEA, $P=0.2487$; DHEAS, $P=0.4740$). Figure 1 depicts the androgen levels for women after dividing the group into responders *vs* nonresponders. Testosterone, DHEA, and DHEAS levels in women responders during treatment were significantly lower than those observed in women nonresponders (testosterone, $P=0.007$; DHEA, $P=0.046$; DHEAS, $P=0.029$). When men were included in the analysis, DHEA and DHEAS levels during treatment in the responders ($n=20$) were still significantly lower than in the nonresponders ($n=44$) (DHEA, $P=0.0324$; DHEAS, $P=0.0447$).

DISCUSSION

The present study of androgen levels (testosterone, DHEA, and DHEAS) in advanced NSCLC patients treated with gefitinib monotherapy revealed treatment-related decrease, especially in women who had no smoking history. The clinical response of gefitinib treatment appeared to be correlated with the suppression of the hormone levels.

To our knowledge, there have been no previous reports of effects of gefitinib treatment on levels of androgens in patients, although a number of authors have examined relationships between androgens and activity of the epidermal growth factor network (Klein and Nielsen, 1993; Dammann *et al*, 2000; Torring *et al*, 2003). There is evidence that EGFR expression is involved in prostate cancer development and in progression to androgen independence (Di Lorenzo *et al*, 2002), and an *in vitro* study has provided evidence that androgens increase the EGFR levels in androgen-sensitive prostate cancer cells and that EGFR signaling is essential for androgen-induced proliferation and survival (Torring *et al*, 2003). Although there has been no indication of any relationship between androgens and EGFR in NSCLCs, expression of ARs has been detected in NSCLC cell lines and biopsy samples of primary lung cancers (Kaiser *et al*, 1996). Additionally, expression has been detected more frequently in women with adenocarcinoma, and thus this may be a prognostic factor for use of gefitinib in NSCLCs (Fukuoka *et al*, 2003; Kris *et al*, 2003; Miller *et al*, 2004). The data suggest that there is a correlation between the AR and EGFR functions in lung cancer. In agreement with this hypothesis, our results demonstrated clinical responses to gefitinib treatment to correlate with suppression of androgen levels.

One reason for lower androgen levels in responders than nonresponders might be that smokers are resistant and have higher androgen levels. However, there were no significant difference in smoking history between responders and non-responder in our study and there was no significant difference of the pretreatment levels of androgens between smokers and nonsmokers. On the other hand, gefitinib treatment significantly suppressed androgen levels in women who had no smoking history, but not in smokers. Smoking may disrupt the correlation between EGFR and androgen.

Both gefitinib and androgens are metabolised by CYP3A4/5; therefore, it can be speculated that gefitinib may affect the metabolisms of androgens. On the other hand, there are no direct evidences demonstrating PK interaction between gefitinib and androgens. PK interaction between gefitinib and other drugs metabolised by CY3A4/5 such as docetaxel or irinotecan were reported (Fandi *et al*, 2003; Furman *et al*, 2004). These reports suggested that gefitinib may decrease the clearance of these drugs and it may be due to CYP3A4/5 substrate competition. If there are any PK interactions between gefitinib and androgens, androgens clearance may decrease and androgen levels may increase by gefitinib treatment. However, we showed that gefitinib treatment decreased the levels of androgens and it suggested that the effect may not be due to change of CYP3A4/5 activity.

With single estimations of testosterone and DHEA, it is necessary to take into account the circadian rhythms. In this study, all blood was therefore taken at approximately the same time, that is, between 10:00 and 14:00, although this does not preclude any influence of cycles. On the other hand, several reports have suggested that there is no circadian rhythm for serum DHEAS levels (Molta and Schwartz, 1986; Hall *et al*, 1993; Kos-Kudla *et al*, 2001). Therefore, the differences seen in the DHEAS levels in this study presumably reflect actual effects of gefitinib treatment. This would suggest that the data for the other hormones might also have clinical significance.

In conclusion, the results of the present small, retrospective study indicate that androgen levels in NSCLC patients are affected by gefitinib treatment and that they may be factors determining sensitivity to this chemotherapeutic agent. Further large-scale prospective trials are needed in the future to confirm these results and to examine inter-relationships among androgens, smoking, gefitinib sensitivity, and EGFR mutations.

ACKNOWLEDGEMENTS

A part of this study was supported by Grants-in-Aid for Scientific Research from the Ministry of Education, Culture, Sports, Science, and Technology of Japan, and Grants-in-Aid for Cancer Research from the Ministry of Health, Labour, and Welfare of Japan.

REFERENCES

Beattie CW, Hansen NW, Thomas PA (1985) Steroid receptors in human lung cancer. *Cancer Res* **45:** 4206–4214

Dammann CE, Ramadurai SM, McCants DD, Pham LD, Nielsen HC (2000) Androgen regulation of signaling pathways in late fetal mouse lung development. *Endocrinology* **141:** 2923–2929

Di Lorenzo G, Tortora G, D'Armiento FP, De Rosa G, Staibano S, Autorino R, D'Armiento M, De Laurentiis M, De Placido S, Catalano G, Bianco AR, Ciardiello F (2002) Expression of epidermal growth factor receptor correlates with disease relapse and progression to androgen-independence in human prostate cancer. *Clin Cancer Res* **8:** 3438–3444

Fandi A, Gatzemeier U, Smith R, Averbuch S, Manegold C (2003) Final data from a pilot trial of gefitinib (ZD1839) in combination with docetaxel in patients with advanced or metastatic non-small-cell lung cancer (NSCLC): Safety and pharmacokinetics. *Proc Am Soc Clin Oncol* **22:** 655

Ferlay J, Bray F, Pisani P, Parkin DM (2001) *GLOBOCAN 2000: Cancer Incidence, Mortality and Prevalence Worldwide, Version 1.0 (IARC, CancerBase No. 5)*. Lyon, France: IARC Press

Fukuoka M, Yano S, Giaccone G, Tamura T, Nakagawa K, Douillard J-Y, Nishiwaki Y, Vansteenkiste J, Kudoh S, Rischin D, Eek R, Horai T, Noda K, Takata I, Smit E, Averbuch S, Macleod A, Feyereislova A, Dong R-P, Baselga J (2003) Multi-institutional randomized phase II trial of gefitinib for previously treated patients with advanced non-small-cell lung cancer. *J Clin Oncol* **21:** 2237–2246

Furman WL, Daw NC, Crews KR, Stewart CF, McCarville B, Santana VM, Hawkins D, Rodriguez-Galindo C, Navid F, Houghton PJ (2004) A phase I study of gefitinib and irinotecan (IRN) in pediatric patients with refractory solid tumors. *Proc Am Soc Clin Oncol* **22:** 8521

Hall GM, Perry LA, Spector TD (1993) Depressed levels of dehydroepiandrosterone sulphate in postmenopausal women with rheumatoid arthritis but no relation with axial bone density. *Ann Rheum Dis* **52:** 211–214

Kaiser U, Hofmann J, Schilli M, Wegmann B, Klotz U, Wedel S, Virmani AK, Wollmer E, Branscheid D, Gazdar AF, Havemann K (1996) Steroid-hormone receptors in cell lines and tumor biopsies of human lung cancer. *Int J Cancer* **67:** 357–364

Klein JM, Nielsen HC (1993) Androgen regulation of epidermal growth factor receptor binding activity during fetal rabbit lung development. *J Clin Invest* **91:** 425–431

Kos-Kudla B, Ostrowska Z, Marek B, Ciesielska-Kopacz N, Kudla M, Kajdaniuk D, Siemidska L, Strzelczyk J (2001) Circadian serum levels of dehydroepiandrosterone sulphate in postmenopausal asthmatic women before and after long-term hormone replacement. *Endocr Regul* **35:** 217–222

Kris MG, Natale RB, Herbst RS, Lynch Jr TJ, Prager D, Belani CP, Schiller JH, Kelly K, Spiridonidis H, Sandler A, Albain KS, Cella D, Wolf MK, Averbuch SD, Ochs JJ, Kay AC (2003) Efficacy of gefitinib, an inhibitor of the epidermal growth factor receptor tyrosine kinase, in symptomatic patients with non-small cell lung cancer: a randomized trial. *JAMA* **290:** 2149–2158

Law MR, Cheng R, Hackshaw AK, Allaway S, Hale AK (1997) Cigarette smoking, sex hormones and bone density in women. *Eur J Epidemiol* **13:** 553–558

Lin P, Chang JT, Ko JL, Liao SH, Lo WS (2004) Reduction of androgen receptor expression by benzo[alpha]pyrene and 7, 8-dihydro-9, 10-epoxy-7, 8, 9, 10-tetrahydrobenzo [alpha] pyrene in human lung cells. *Biochem Pharmacol* **67:** 1523–1530

Lynch TJ, Bell DW, Sordella R, Gurubhagavatula S, Okimoto RA, Brannigan BW, Harris PL, Haserlat SM, Supko JG, Haluska FG, Louis DN, Christiani DC, Settleman J, Haber DA (2004) Activating mutations in the epidermal growth factor receptor underlying responsiveness of non-small-cell lung cancer to gefitinib. *N Engl J Med* **350:** 2129–2139

Miller VA, Kris MG, Shah N, Patel J, Azzoli C, Gomez J, Krug LM, Pao W, Rizvi N, Pizzo B, Tyson L, Venkatraman E, Ben-Porat L, Memoli N, Zakowski M, Rusch V, Heelan RT (2004) Bronchioloalveolar pathologic subtype and smoking history predict sensitivity to gefitinib in advanced non-small-cell lung cancer. *J Clin Oncol* **22:** 1103–1109

Molta L, Schwartz U (1986) Gonadal and adrenal androgen secretion in hirsute females. *Clin Endocrinol Metab* **15:** 229–245

Non-Small Cell-Lung Cancer Collaborative Group (1995) Chemotherapy in non-small cell lung cancer: a meta-analysis using updated data on individual patients from 52 randomised clinical trials. Non-small Cell Lung Cancer Collaborative Group. *BMJ* **311:** 899–909

Paez JG, Janne PA, Lee JC, Tracy S, Greulich H, Gabriel S, Herman P, Kaye FJ, Lindeman N, Boggon TJ, Naoki K, Sasaki H, Fujii Y, Eck MJ, Sellers WR, Johnson BE, Meyerson M (2004) EGFR mutations in lung cancer: correlation with clinical response to gefitinib therapy. *Science* **304:** 1497–1500

Pao W, Miller V, Zakowski M, Doherty J, Politi K, Sarkaria I, Singh B, Heelan R, Rusch V, Fulton L, Mardis E, Kupfer D, Wilson R, Kris M, Varmus H (2004) EGF receptor gene mutations are common in lung cancers from 'never smokers' and are associated with sensitivity of tumors to gefitinib and erlotinib. *Proc Natl Acad Sci USA* **101:** 13306–13311

Schiller JH, Harrington D, Belani CP, Langer C, Sandler A, Krook J, Zhu J, Johnson DH (2002) Comparison of four chemotherapy regimens for advanced non-small-cell lung cancer. *N Engl J Med* **346:** 92–98

Torring N, Dagnaes-Hansen F, Sorensen BS, Nexo E, Hynes NE (2003) ErbB1 and prostate cancer: ErbB1 activity is essential for androgen-induced proliferation and protection from the apoptotic effects of LY294002. *Prostate* **56:** 142–149

Trummer H, Habermann H, Haas J, Pummer K (2002) The impact of cigarette smoking on human semen parameters and hormones. *Hum Reprod* **17:** 1554–1559

Wakeling AE, Guy SP, Woodburn JR, Ashton SE, Curry BJ, Barker AJ, Gibson KH (2002) ZD1839 (Iressa): an orally active inhibitor of epidermal growth factor signaling with potential for cancer therapy. *Cancer Res* **62:** 5749–5754

WHO (1979) *World Health Organization: WHO Handbook for Reporting Results of Cancer Treatment*, Vol 48, Geneva, Switzerland: WHO Offset Publication

Int. J. Cancer: **116,** 36–44 (2005)

Establishment of a human non-small cell lung cancer cell line resistant to gefitinib

Fumiaki Koizumi[1,3], Tatsu Shimoyama[1,4], Fumiko Taguchi[1,4], Nagahiro Saijo[2] and Kazuto Nishio[1,4]*
[1]*Shien-Lab, National Cancer Center Hospital, Tokyo, Japan*
[2]*Medical Oncology Department, National Cancer Center Hospital, Tokyo, Japan*
[3]*Investigative Treatment Division, National Cancer Center Research Institute EAST, Kashiwa, Japan*
[4]*Pharmacology Division, National Cancer Center Research Institute, Tokyo, Japan*

The epidermal growth factor receptor (EGFR) tyrosine-kinase inhibitor gefitinib (Iressa®, ZD1839) has shown promising activity preclinically and clinically. Because comparative investigations of drug-resistant sublines with their parental cells are useful approaches to identifying the mechanism of gefitinib resistance and select factors that determine sensitivity to gefitinib, we established a human non-small cell lung carcinoma subline (PC-9/ZD) that is resistant to gefitinib. PC-9/ZD cells are ~180-fold more resistant to gefitinib than their parental PC-9 cells and PC-9/ZD cells do not exhibit cross-resistance to conventional anticancer agents or other tyrosine kinase inhibitors, except AG-1478, a specific inhibitor of EGFR. PC-9/ZD cells also display significant resistance to gefitinib in a tumor-bearing animal model. To elucidate the mechanism of resistance, we characterized PC-9/ZD cells. The basal level of EGFR in PC-9 and PC-9/ZD cells was comparable. A deletion mutation was identified within the kinase domain of *EGFR* in both PC-9 and PC-9/ZD, but no difference in the sequence of *EGFR* cDNA was detected in either cell line. Increased EGFR/HER2 (and EGFR/HER3) heterodimer formations were demonstrated in PC-9/ZD cells by chemical cross-linking and immunoprecipitation analysis in cells unexposed to gefitinib. Exposure to gefitinib increased heterodimer formation in PC-9 cells, but not in PC-9/ZD cells. Gefitinib inhibits EGFR autophosphorylation in a dose-dependent manner in PC-9 cells but not in PC-9/ZD cells. A marked difference in inhibition of site-specific phosphorylation of EGFR was observed at Tyr1068 compared to other tyrosine residues (Tyr845, 992 and 1045). To elucidate the downstream signaling in the PC9/ZD cellular machinery, complex formation between EGFR and its adaptor proteins GRB2, SOS, and Shc was examined. A marked reduction in the GRB2-EGFR complex and absence of SOS-EGFR were observed in PC-9/ZD cells, even though the protein levels of GRB2 and SOS in PC-9 and PC-9/ZD cells were comparable. Expression of phosphorylated AKT was increased in PC-9 cells and inhibited by 0.02 μM gefitinib. But the inhibition was not significant in PC-9/ZD cells. These results suggest that alterations of adaptor-protein-mediated signal transduction from EGFR to AKT is a possible mechanism of the resistance to gefitinib in PC-9/ZD cells. These phenotypes including EGFR–SOS complex and heterodimer formation of HER family members are potential biomarkers for predicting resistance to gefitinib.

Key words: resistance; gefitinib; EGFR; Grb2; SOS; non-small cell lung cancer

Chemotherapy has played a central role in the treatment of patients with inoperable NSCLC for over 30 years, although its efficacy seems to be of very limited value.[1,2] Human solid tumors, including lung cancer, glioblastoma, breast cancer, prostate cancer, gastric cancer, ovarian cancer, cervical cancer and head and neck cancer, express epidermal growth factor receptor (EGFR) frequently, and elevated EGFR levels are related to disease progression, survival, stage and response to therapy.[2–10] The therapies directed at blocking EGFR function are attractive.

Interest in target-based therapy has been growing ever since the clinical efficacy of STI-571 was first demonstrated,[11–13] and small molecules and monoclonal antibodies that block activation of the EGFR and HER2 have been developed over the past few decades. The leading small-molecule EGFR tyrosine-kinase inhibitor, gefitinib (Iressa®, ZD1839), has shown excellent antitumor activity in a series of Phase I and II studies,[14,15] and Phase II international multicenter trials (Iressa Dose Evaluation in Advanced Lung Cancer (IDEAL) 1 and 2) yield an overall RR of 11.8–18.4% and overall disease control rate of 42.2–54.4% (gefitinib 250 mg/day) in patients with advanced non-small cell lung cancer (NSCLC) who had undergo at least 2 previous treatments with chemotherapy. INTACT 1 and 2 ('Iressa' NSCLC Trials Assessing Combination Therapy) have demonstrated that gefitinib does not provide improvement in survival when added to standard first line platinum-based chemotherapy *vs.* chemotherapy alone in advanced NSCLC.[16,17] Two small retrospective studies reported recently that activating mutation of *EGFR* correlate with sensitivity and clinical response to gefitinib and erlotinib.[18–20] Although information of *EGFR* mutation may enable to identify the subgroup of patients with NSCLC who will respond to gefitinib and erlotinib, it would be expected that acquired resistance would develop in such patients after treatment. The problem of acquired resistance to gefitinib might be growing, but there has been no preclinical research about the mechanism of developing resistance to gefitinib. We established resistant subline using PC-9 that is highly sensitive to gefitinib.

Establishment of drug-resistant sublines and comparative investigations with their parental cells to identify their molecular, biological and biochemical properties are useful approaches to elucidating the mechanism of the drug's action. Our study describes the establishment of a gefitinib-resistant cell line and its characterization at the cellular and subcellular levels. The PC-9/ZD cell line is the first human NSCLC cell line resistant to gefitinib ever reported. PC-9 is a lung adenocarcinoma cell line that is highly sensitive to gefitinib at its IC_{50}-value of 0.039 μM, but the PC-9/ZD subline, which has a level of EGFR expression comparable to that of PC-9 cells, is specifically resistant to gefitinib. Thus, PC-9 and PC-9/ZD cells will provide useful information about the mechanism of developing resistance to gefitinib and molecules as surrogate markers for predicting chemosensitivity to gefitinib.

Material and methods

Drugs and cells

Gefitinib(*N*-(3-chloro-4-fluorophenyl)-7-methoxy-6-[3-(morpholin-4-yl)propoxy] quinazolin-4-amine) was supplied by AstraZeneca Pharmaceuticals (Cheshire, UK). AG-1478, AG-825, K252a, staurosporin, genistein, RG-14620 and Lavendustin A were purchased from Funakoshi Co. Ltd (Tokyo, Japan).

NSCLC cell line PC-9 (derived from a patient with adenocarcinoma untreated previously) was provided by Prof. Hayata of Tokyo Medical University (Tokyo, Japan).[21] PC-9 and PC-9/ZD cells were cultured in RPMI-1640 medium (Sigma, St. Louis, MO) supplemented with 10% FBS (GIBCO-BRL, Grand Island, NY), penicillin and streptomycin (100 U/ml and 100 μg/ml, respectively; GIBCO-BRL) in a humidified atmosphere of 5%

***Correspondence to:** Shien-Lab, Medical Oncology Department, National Cancer Center Hospital, 5-1-1 Tsukiji, Chuo-ku, Tokyo, 104-0045, Japan. Fax: +81-3-3547-5185. E-mail: knishio@gan2.res.ncc.go.jp
Received 1 July 2004; Accepted after revision 21 December 2004
DOI 10.1002/ijc.20985
Published online 10 March 2005 in Wiley InterScience (www.interscience.wiley.com).

CO_2 at 37°C. Gefitinib-resistant PC-9/ZD cells were selected from a subculture that had acquired resistance to gefitinib using the following procedure. Cultured PC-9 cells were exposed to 2.5 μg/ml *N*-methyl-*N'*-nitro-*N*-nitrosoguanidine (MNNG) for 24 hr and then washed and cultured in medium containing 0.2 μM gefitinib for 7 days. After exposure to gefitinib, they were washed and cultured in drug-free medium for 14 days. When variable cells had increased, they were seeded in medium containing 0.3–0.5 μM of gefitinib on 96-well cultured plates for subcloning. After 21–28 days, the colonies were harvested and a single clone was obtained. The subcloned cells exhibited an 182-fold increase in resistance to the growth-inhibitory effect of gefitinib as determined by MTT assay, and the resistant phenotype has been stable for at least 6 months under drug-free conditions.

In vitro *growth-inhibition assay*

The growth-inhibitory effects of cisplatin, carboplatin, adriamycin, irinotecan, gemcitabine, vindesine, paclitaxel, genistein, K252a, staurosporin, AG-825, AG-1478, Tyrophostin 51, RG-14620, Lavendustin A and gefitinib in PC-9 and PC-9/ZD cells were examined by using a 3-(4,5-dimethylthiazol-2-yl)- 2,5-diphenyltetrazolium bromide (MTT) assay.[22] A 180 μl volume of an exponentially growing cell suspension (6×10^3 cells/ml) was seeded into a 96-well microtiter plate, and 20 μl of various concentrations of each drug was added. After incubation for 72 hr at 37°C, 20 μl of MTT solution (5 mg/ml in PBS) was added to each well, and the plates were incubated for an additional 4 hr at 37°C. After centrifuging the plates at 200*g* for 5 min, the medium was aspirated from each well and 180 μl of DMSO was added to each well to dissolve the formazan. Optical density was measured at 562 and 630 nm with a Delta Soft ELISA analysis program interfaced with a Bio-Tek Microplate Reader (EL-340, Bio-Metallics, Princeton, NJ). Each experiment was carried out in 6 replicate wells for each drug concentration and carried out independently 3 or 4 times. The IC_{50}-value was defined as the concentration needed for a 50% reduction in the absorbance calculated based on the survival curves. Percent survival was calculated as: (mean absorbance of 6 replicate wells containing drugs − mean absorbance of six replicate background wells)/(mean absorbance of 6 replicate drug-free wells − mean absorbance of 6 replicate background wells) × 100.

In vivo *growth-inhibition assays*

Experiments were carried out in accordance with the United Kingdom Coordinating Committee on Cancer Research Guidelines for the welfare of animals in experimental neoplasia (2nd ed.). Female BALB/c nude mice, 6-weeks-old, were purchased from Japan Charles River Co. Ltd (Atsugi, Japan). All mice were maintained in our laboratory under specific-pathogen-free conditions. *In vivo* experiments were scheduled to evaluate the effect of oral administration of gefitinib on pre-existing tumors. Ten days before administration, 5×10^6 PC-9 or PC-9/ZD cells were injected subcutaneously (s.c.) into the back of the mice, and gefitinib (12.5, 25 or 50 mg/kg, p.o.) was administered to the mice on Days 1–21. Tumor diameter was measured with calipers on Days 1, 4, 8, 11, 14, 19 and 22 to evaluate the effect of treatment, and tumor volume was determined by using the following equation: tumor volume = $ab^2/2$ (mm^3) (where *a* is the longest diameter of the tumor and *b* is the shortest diameter). Day "x" denotes the day on which the effect of the drugs was estimated, and Day "1" denotes the first day of treatment. All mice were sacrificed on Day 22, after measuring their tumors. We considered absence of a tumor mass on Day 22 to indicate a cure. Differences in tumor sizes between the treatment groups and control group at Day 22 were analyzed by the unpaired *t*-test. A *p*-value of <0.05 was considered statistically significant.

cDNA expression array

The gene expression profile of PC-9/ZD was assessed with an Atlas Nylon cDNA Expression Array (BD Bioscience Clontech, Palo Alto, CA). Total RNA was extracted by a single-step guanidinium thiocyanate procedure (ISOGEN, Nippon Gene, Tokyo, Japan). An Atlas Pure Total RNA Labeling System was used to isolate RNA and label probes. The materials provided with the kit were used, and the manufacturer's instructions were followed for all steps. Briefly, streptavidin-coated magnetic beads and biotinylated oligo(dT) were used to isolate poly A RNA from 50 μg of total RNA and the RNA obtained was converted into ^{32}P-labeled first-strand cDNA with MMLV reverse transcriptase. The ^{32}P-labeled cDNA fraction was purified on NucleoSpin columns and was added to the membrane on which fragments of 777 genes were spotted. Hybridization was allowed to proceed overnight at 68°C. After washing, the radiolabeled spots were visualized and quantified by BAS-2000II and Array Gauge 1.1 (Fuji Film Co., Ltd., Tokyo, Japan). The data were adjusted for the total density level of each membrane.

Quantitative real-time RT-PCR analysis

Total RNAs extracted from PC-9 cells and PC-9/ZD cells (1×10^6 cells each) were incubated with DNase I (Invitrogen, Carlsbad, CA) for 30 min. First-strand cDNA synthesis was carried out on 1 μg of RNA in 10 μl of a reaction mixture with 50 pmol of Random hexamers and 50 U of M-MLV RTase. Oligonucleotide primers for human *EGFR* were obtained from Takara (HA003051, Takara Bio Co., Tokyo, Japan). For PCR calibration, we generated a calibrator dilution series for *EGFR* cDNA in pUSEamp vector (Upstate, Charlottesville, VA) ranging from 10^8–10^2 copies/1 μl. A total of 2 μl of reverse transcriptase products was used for PCR amplification using Smart Cycler system (Takara) according to manufacturer's instructions. Absolute copy numbers were calculated back to the initial cell numbers, which were set into the RNA extraction. As a result we obtained copies/cell:ratio representing the average *EGFR* RNA amount per cell.

Immunoprecipitation and immunoblotting

The cultured cells were washed twice with ice-cold PBS, and lysed in EBC buffer (50 mM Tris-HCl, pH 8.0, 120 mM NaCl, 0.5% Nonidet P-40, 100 mM NaF, 200 mM Na orthovanadate, and 10 mg/ml each of leupeptin, aprotinin, pepstatin A and phenylmethylsulphonyl fluoride). The lysate was cleared by centrifugation at 15,000 r.p.m. for 10 min, and the protein concentration of the supernatant was measured by BCA protein assay (Pierce, Rockford, IL). The membrane was probed with antibody against EGFR (1005; Santa Cruz, Santa Cruz, CA), HER2/neu (c-18; Santa Cruz), HER3 (c-17; Santa Cruz), HER4 (c-18; Santa Cruz), PI3K (4; BD), Grb2 (81; BD), SOS1/2 (D-21; Santa Cruz), Shc (30; BD, San Jose, CA), PTEN (9552; Cell Signaling, Beverly, MA), AKT (9272; Cell Signaling), phospho-EGFR specific for Tyr 845, Tyr 992, Tyr 1045, and Tyr 1068 (2231, 2235, 2237, 2234; Cell Signaling), phospho-AKT (Ser473) (9271; Cell Signaling), phospho-Erk (9106; Cell Signaling), and phospho-Tyr (PY-20; BD) as the first antibody, and then with by horseradish-peroxidase-conjugated secondary antibody. The bands were visualized by enhanced chemiluminescence (ECL Western Blotting Detection Kit, Amersham, Piscataway, NJ). For Immunoprecipitation, 5×10^6 cells were washed, lysed in EBC buffer, and centrifuged, and the supernatants obtained (1,500 μg) were incubated at 4°C with the anti-EGFR (1005), -HER2 (c-18), and -HER3 (c-17) Ab overnight. The immunocomplexes were absorbed onto protein A/G-Sepharose beads, washed 5 times with lysate buffer, denatured, and subjected to electrophoresis on a 7.5% polyacrylamide gel.

Analysis of the genes of the HER families by direct sequencing

Total RNAs were extracted from PC-9 and PC-9/ZD cells with ISOGEN (Nippon Gene) according to manufacturer's instructions. First-strand cDNA was synthesized from 2 μg of total RNA by using 400 U of SuperScript II (Invitrogen, Carlsbad, CA). After reverse transcription with oligo (dT) primer (Invitrogen) or random primer (Invitrogen), the first-strand cDNA was amplified by PCR by using specific primers for *EGFR*, *HER2* and *HER3*. The

reaction mixture (50 μl) contained 1.25 U AmpliTaq DNA polymerase (Applied Biosystem, Foster City, CA), and amplification was carried out by 30 cycles of denaturation (95°C, 30 sec), annealing (55–59°C, 30 sec), and extension (72°C, 30 sec) with a GeneAmp PCR System 9600 (Applied Biosystem). After amplification, 5 μl of the RT-PCR products was subjected to electrophoretic analysis on a 2% agarose gel with ethidium bromide. DNA sequencing of the PCR products was carried out by the dideoxy chain termination method using the ABI PRISM 310 Genetic Analyzer (Applied Biosystem).

Chemical cross-linking

Chemical cross-linking in intact cells was carried out as described previously.[23] In brief, after 6 hr exposure to 0.2 μM gefitinib, cells were washed with PBS and incubated for 25 min at 4°C in PBS containing 1.5 mM of the nonpermeable cross-linker bis (sulfosuccinimidyl) substrate (Pierce, Rockford, IL). The reaction was terminated by adding 250 mM glycine for 5 min while rocking. Cells were washed in EBC buffer and 20 μg of protein was resolved by 5–10% gradient SDS-PAGE, and then immunoblot analyzed for EGFR, HER2, HER3 and P-Tyr.

Results

Sensitivity of PC-9/ZD cells to cytotoxic agents and tyrosine kinase inhibitors

No significant difference between PC-9 and PC-9/ZD cells was observed in *in vitro* cell growth (doubling time of 20.3 hr and 21.4 hr, respectively) and microscopic morphology. Figure 1 shows the growth-inhibitory effect of gefitinib on the parent PC-9 cell line and its resistant subline, PC-9/ZD. The IC_{50}-value of gefitinib in PC-9 cells was 0.039 μM, as compared to 7.1 μM in PC-9/ZD cells (182-fold resistance). PC-9/ZD cells exhibited no cross-resistance to other conventional anticancer agents, including cisplatin, carboplatin, adriamycin, vindesine, paclitaxel and irinotecan. We also examined the growth-inhibitory effect of the EGFR tyrosine kinase inhibitors AG-1478, RG-14620 and Lavendustin A and other tyrosine kinase inhibitors in PC-9 and PC-9/ZD cells. PC-9/ZD cells show cross-resistance to AG1478, but not to all of the tyrosine kinase inhibitors (Tables I, II). It is likely that PC-9/ZD would also be resistant to EGFR-targeted quinazoline derivatives including gefitinib and erlotinib.[20]

PC-9/ZD cells show significant resistance to gefitinib in an in vivo *model*

To ascertain whether the resistance of PC-9/ZD occurs *in vivo*, we investigated the growth-inhibitory effect of gefitinib on PC-9 cells and PC-9/ZD cells in a xenotransplanted model. There was no significant difference in the size of the of PC-9 and PC-9/ZD cell tumor masses in nude mice before the start of gefitinib injection. Figure 2 shows the growth-inhibition curve of PC-9 (Fig. 2*a*) and PC-9/ZD (Fig. 2*b*) cells *in vivo* during the observation period. The PC-9 tumor masses decreased markedly in volume at all doses of gefitinib. In the 50 mg/kg/day p.o. group, the PC-9 masses were eradicated in all mice and did not regrow within the observation period. Growth of the PC-9/ZD masses, on the other hand, was inhibited by gefitinib administration in a dose-dependent manner, but significant tumor reduction was observed only in the 25 and 50 mg/kg/day groups, and the PC-9/ZD masses were not eradicated even in 50 mg/kg/day group. These results clearly demonstrate the significant *in vivo* resistance of PC-9/ZD cells to gefitinib.

Expression of HER family members and related molecules in PC-9 and PC-9/ZD cells

We examined the gene expression and protein levels of HER family members and related molecules by cDNA expression array (followed by confirmation using RT-PCR, data not shown) and immunoblotting. The ratios of the protein expression levels of PC-9 cells to PC-9/ZD cells almost paralleled the expression levels of their genes (Fig. 3*a*). The basal level of EGFR was comparable or slightly higher in PC-9/ZD cells (Fig. 3*a,b*), whereas the HER3 and AKT levels were lower in resistant cells.

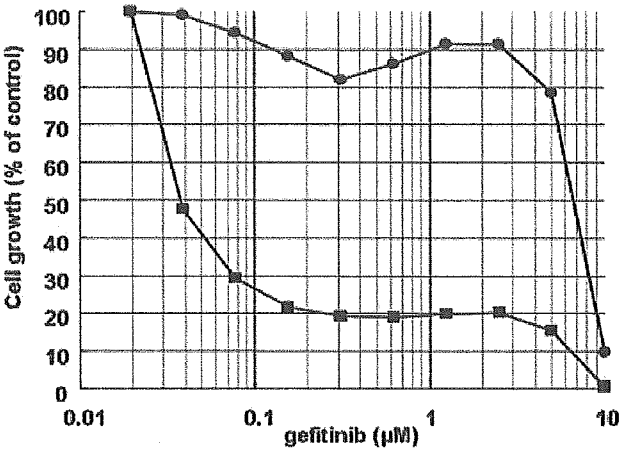

	PC-9	PC-9/ZD
IC_{50} value (μM)	0.039± 0.002	7.1± 0.06
Doubling time (hr)	20.3	21.0

FIGURE 1 – Growth-inhibitory effect of gefitinib on PC-9 and PC-9/ZD cells determined by MTT assay. The cells were exposed to the concentrations of gefitinib indicated for 72 hr. The growth–inhibition curves of PC-9 (■) and PC-9/ZD (●) are shown. Doubling time was determined by MTT assay.

TABLE I – CHEMOSENSITIVITY TO OTHER ANTICANCER DRUGS

Drug	IC_{50} values (μM)[1]		RR[2] 1.6
	PC-9	PC-9/ZD	
Cisplatin	1.9 ± 0.7	3.1 ± 1.5	2.0
Carboplatin	25 ± 21	49 ± 23	1.3
Adriamycin	0.16 ± 0.13	0.20 ± 0.15	2.2
Irinotecan	15 ± 10	32 ± 11	1.5
Etoposide	4.5 ± 1.5	6.6 ± 1.3	1.5
Gemcitabine	18 ± 1.5	27 ± 1.5	0.7
Vindesine	0.0046 ± 0.0004	0.0032 ± 0.0009	1.2
Paclitaxel	0.0041 ± 0.0011	0.0048 ± 0.0004	1.6

[1]As assessed by MTT assay in PC-9 and PC-9/ZD cells. Values are the mean ± SD of >3 independent experiments.–[2]Relative resistance value (IC_{50} of resistant cells/IC_{50} of parental cells).

We carried out quantitative RT-PCR to measure the copy numbers of *EGFR*. Estimated transcript levels of *EGFR* were 786.3 and 712.1 copies/cell for PC-9 cells and PC-9/ZD cells, respectively (Fig. 3*d*). Relative ratio of *EGFR* expression levels in PC-9 cells and PC-9/ZD cells is 1.104. Microarray analysis using CodeLink Bioarray (Amersham Bio, Piscataway, NJ) confirmed equivalent gene expression of *EGFR* with ratio of 1.002 between PC-9 and PC-9/ZD cells (data not shown).

Expression of PI3K, Grb2, SOS, and Shc, the adaptor proteins of EGFR, and PTEN was almost the same in PC-9 and PC-9/ZD cells, and no change in the protein levels was observed after exposure to gefitinib (data not shown). The relative densitometric units of each protein are shown in Figure 3*c*. These results suggest that the difference in protein levels of EGFR, HER2, and related proteins can not explain the high resistance of PC-9/ZD cells to gefitinib.

Sequence of HER family member in PC-9/ZD cells

Several reports suggest that the resistance to receptor tyrosine kinase inhibitor STI-571 is partially due to mutations in the

TABLE II – CHEMOSENSITIVITY TO PROTEIN KINASE INHIBITORS[1]

Inhibitor	Target	IC_{50} values (μM)		RR[2]
		PC-9	PC-9/ZD	
AG-1478	EGFR	0.052 ± 0.02	6.0 ± 0.8	117
RG-14620	EGFR	13 ± 1.0	13 ± 2.5	1.0
Lavendustin A	EGFR	20 ± 4.6	27 ± 2.6	1.3
Genistein	TK	18 ± 1.5	27 ± 1.5	1.5
K252a	PKC	0.47 ± 0.17	0.63 ± 0.04	1.3
Staurosporin	PKC	0.0036 ± 0.0019	0.004 ± 0.0014	1.1
AG-825	HER2	>50	>50	

[1]Assessed by MTT assay in PC-9 and PC-9/ZD cells. Values are the mean ± SD of >3 independent experiments.–[2]Relative resistance value (IC_{50} of resistant cells/IC_{50} of parental cells).

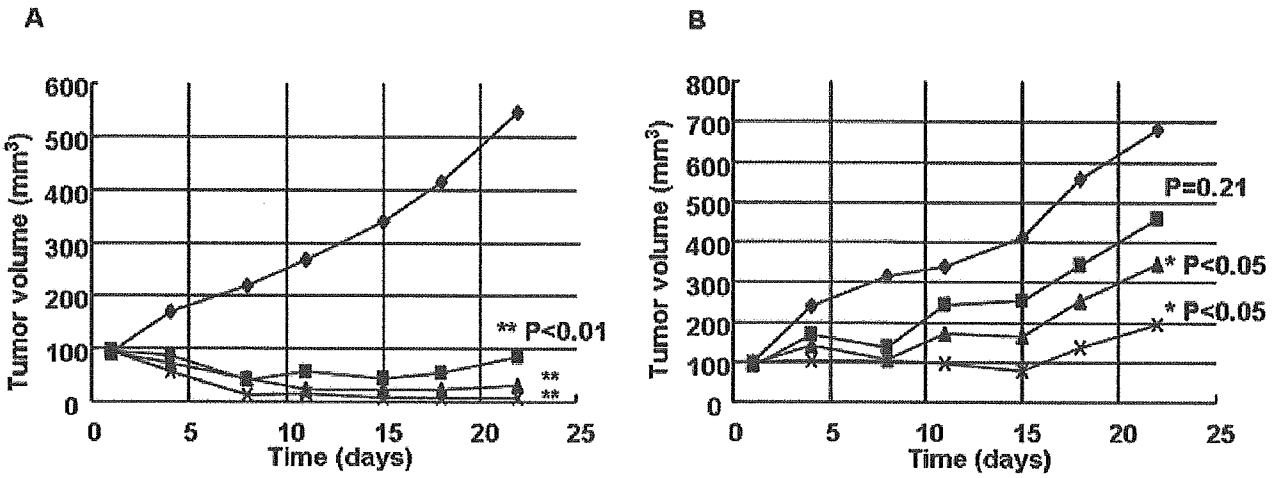

FIGURE 2 – Growth-inhibitory effect of gefitinib on PC-9 and PC-9/ZD cells xenotransplanted into nude mice. Ten days before gefitinib administration, 5×10^6 PC-9 (*a*) or PC-9/ZD (*b*) cells were injected s.c. into the back of mice. The mice were divided into 4 groups (◆, control group; ■, 12.5 mg/Kg group; ▲, 25 mg/Kg group; ×, 50 mg/Kg group). Gefitinib was administered p.o. to the tumor-inoculated mice on Days 1–21. Each group consisted of 6 mice. The statistical analysis was carried out by using the unpaired *t*-test.

ATP-binding site of the Bcr-Abl, the target of the drug.[24–27] We analyzed the sequences of the cDNAs of *EGFR*, *HER2*, and *HER3*, but found no differences in their sequences between PC-9 and PC-9/ZD cells. We did detect a deleted position of *EGFR* in both cell lines that results in deletion of 5 amino acids (Glu722, Leu723, Arg724, Glu725, and Ala726) (Fig. 4). Our findings indicate that the deletion does not directly contribute to the cellular resistance.

Inhibitory effect of gefitinib on autophosphorylation of EGFR in PC-9/ZD cells

Phosphorylation of EGFR is necessary for EGFR-mediated intracellular signaling. Although the EGFR phosphorylation levels of tumors were thought to be correlated with sensitivity to gefitinib, the basal level of phosphorylated EGFR in PC-9 and PC-9/ZD cells is almost the same. Gefitinib inhibited EGFR autophosphorylation in a dose-dependent manner and completely inhibited its phosphorylation at 0.2–2 μM in PC-9 cells (Fig. 5*a*), but its inhibitory effect on autophosphorylation of EGFR in PC-9/ZD cells was less than in PC-9 cells (Fig. 5*a*). Because each phosphorylation site of EGFR has a different role in the activation of downstream signaling molecules, we examined the inhibitory effect of gefitinib on site-specific phosphorylation of EGFR. Phosphorylation of several different EGFR tyrosine residues (Tyr845, Tyr992 and Tyr1068) was dose-dependently inhibited by gefitinib in PC-9 cells, whereas no clear inhibitory effects of gefitinib on phosphorylation at Tyr 845 and Tyr1068 residues in PC-9/ZD cells was observed (Fig. 5*b,c,e*). The most marked difference of in inhibition between the cells was observed at Tyr1068 (Fig. 5*e*). Tyr1045 showed resistance to inhibition of autophosphorylation by gefitinib in both PC-9 and PC-9/ZD cells (Fig. 5*d*).

Complex formation of EGFR and its adaptor proteins

Tyr1068 of EGFR is the tyrosine that is most resistant to inhibition of autophosphorylation by gefitinib in PC-9/ZD cells. Because the Tyr 1068 is a direct binding site for the GRB2/SH2 domain, and its phosphorylation is related to the complex formation of EGFR-adaptor proteins and their signaling, we examined complex formation between EGFR and the adaptor proteins GRB2, SOS, Shc, and PI3K by immunoprecipitation. The level of expression of these proteins in PC-9 and PC-9/ZD cells were similar (Fig. 3*a*). A smaller amount of EGFR-GRB2 complex was observed in PC-9/ZD cells and no EGFR-SOS complex was detected at all (Fig. 6). The amount of HER2- or HER3-GRB2 complex in PC-9 and PC-9/ZD cells was similar, and no decreases in complex formation were observed after exposure to gefitinib. A decreased amount of HER2-SOS complex and inability to detect HER3-SOS complex were also observed in PC-9/ZD cells. HER2-PI3K complex increased in PC-9/ZD. There are no significant differences in complex formation between SHC and EGFR, HER2, or HER3 between PC-9 and PC-9/ZD cells. These results suggest that GRB2-SOS-mediated signaling may be inactivated in PC-9/ZD cells.

Heterodimerization of HER family member in PC-9/ZD cells

Dimerization of members of the HER family is essential for activation of their catalytic activity and their signaling. We examined the effect of gefitinib on the dimerization of HER family members by immunoblotting, immunoprecipitation and chemical cross-linking analysis (Figs. 3*a*, 5*a*, 7*a*). The expression levels of EGFR and HER2 were similar and the HER3 level was lower in PC-9/ZD cells by immunoblotting (Fig. 3*a*). A chemical cross-

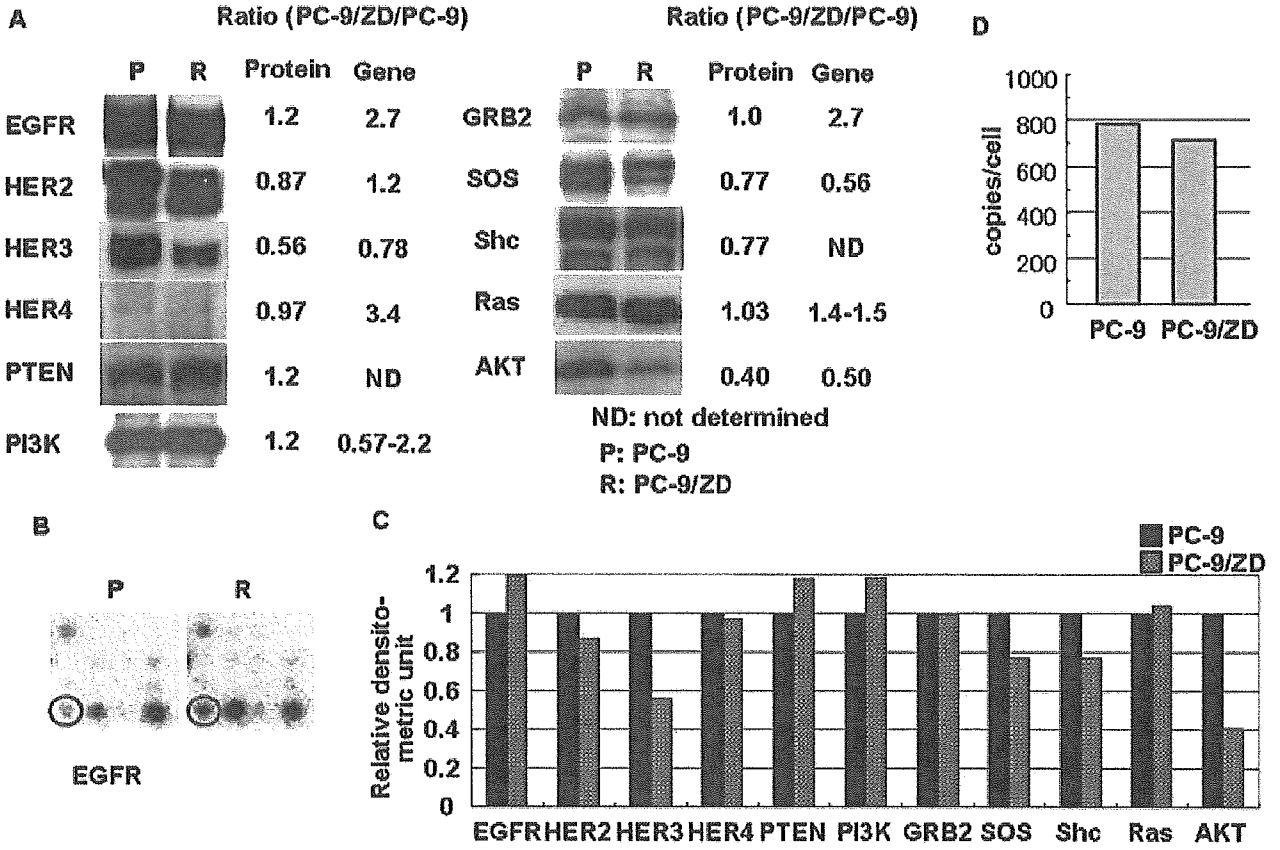

FIGURE 3 – Expresssion of HER family members and related molecules in PC-9 (P) and PC-9/ZD (R) cells. (*a*) Western blot analysis; a 20 μg sample of total cell lysates was separated by SDS-PAGE, transferred to a PVDF membrane, and incubated with a specific anti-human antibody as the first antibody and then with horseradish peroxidase-conjugated secondary antibody. The ratios of the levels of expression of proteins and genes in PC-9 cells to the levels in PC-9/ZD cells are shown. (*b*) cDNA expression array; Poly A RNA was converted into ^{32}P-labeled first-strand cDNA with MMLV reverse transcriptase. The ^{32}P-labeled cDNA fraction was hybridized to the membrane on which fragments of 777 genes were spotted. The close-up view shows *EGFR* mRNA expression. (*c*) Each band was quantified by a densitometry and with NIH image software. The levels of protein expression are shown in a graph. (*d*) Absolute amounts of *EGFR* transcripts of PC-9 cells and PC-9/ZD cells measured by real-time quantitative RT-PCR. The values were calculated back to the initial cell numbers for RNA extraction in Material and Methods.

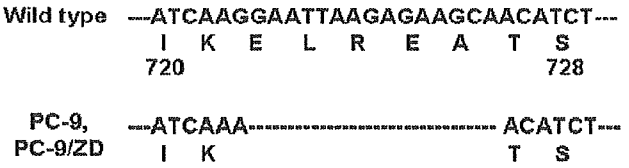

FIGURE 4 – Detection of a deleted position of EGFR. Direct sequencing of a PC-9 and PC-9/ZD-derived, amplified cDNA fragment containing the ATP-binding site of EGFR. *Top*, wild-type EGFR; *bottom*, PC-9 and PC-9/ZD.

linking assay showed that in the absence of gefitinib the amount of high molecular weight complexes (~400 kDa) that are recognized by anti-EGFR antibody (EGFR dimers), including formations of homodimers and heterodimers (EGFR-EGFR, EGFR-HER2 or EGFR-HER3), was almost the same in PC-9 and PC-9/ZD cells, whereas HER2 dimerization detected by anti-HER2 antibody was remarkably lower in PC-9/ZD cells (Fig. 7*a*). Increased EGFR/HER2 (and EGFR/HER3) heterodimer formation was detected in PC-9/ZD cells by immunoprecipitation analysis (Fig. 5*a*). The proportion of EGFR heterodimer to homodimer is increased significantly in PC-9/ZD (Fig. 7*b*). When exposed to gefitinib at a concentration of 0.2 μM for 6 hr the amount of dimer-formation increased similarly in PC-9 and PC-9/ZD cells (Fig. 7*a*), whereas marked induction of hetero-dimerization of EGFR-HER2 was observed only in PC-9 cells (Fig. 5*a*). These results suggest that a difference in hetero- or homo-dimerization is a possible determinant factor of gefitinib sensitivity.

AKT and MAPK pathways in PC-9/ZD cells

Because phosphorylation at Tyr 1068 of EGFR plays an important role for transduction of the signal to downstream of MAPK and AKT pathway,[28,29] we examined the difference between PC-9 and PC-9/ZD cells in downstream signaling. The basal level of phosphorylated AKT is higher in PC-9 cells than in PC-9/ZD cells, and although gefitinib inhibited AKT phosphorylation in a dose-dependent manner (Fig. 8*a*), the inhibitory effect of gefitinib on phosphorylation of AKT in PC-9/ZD cells was significantly less than in PC-9 cells (Fig. 8*a*). This difference in the inhibitory effect of gefitinib on AKT phosphorylation between PC-9 and PC-9/ZD cells is very similar to the difference in effect on EGFR autophosphorylation. No inhibition of phosphorylation of MAPK by gefitinib was observed in either cell line (Fig. 8*b*). These results suggest that downregulation of activated AKT is closely correlated with the cellular sensitivity to gefitinib, but that inhibition of the MAPK pathway does not contribute to drug sensitivity.

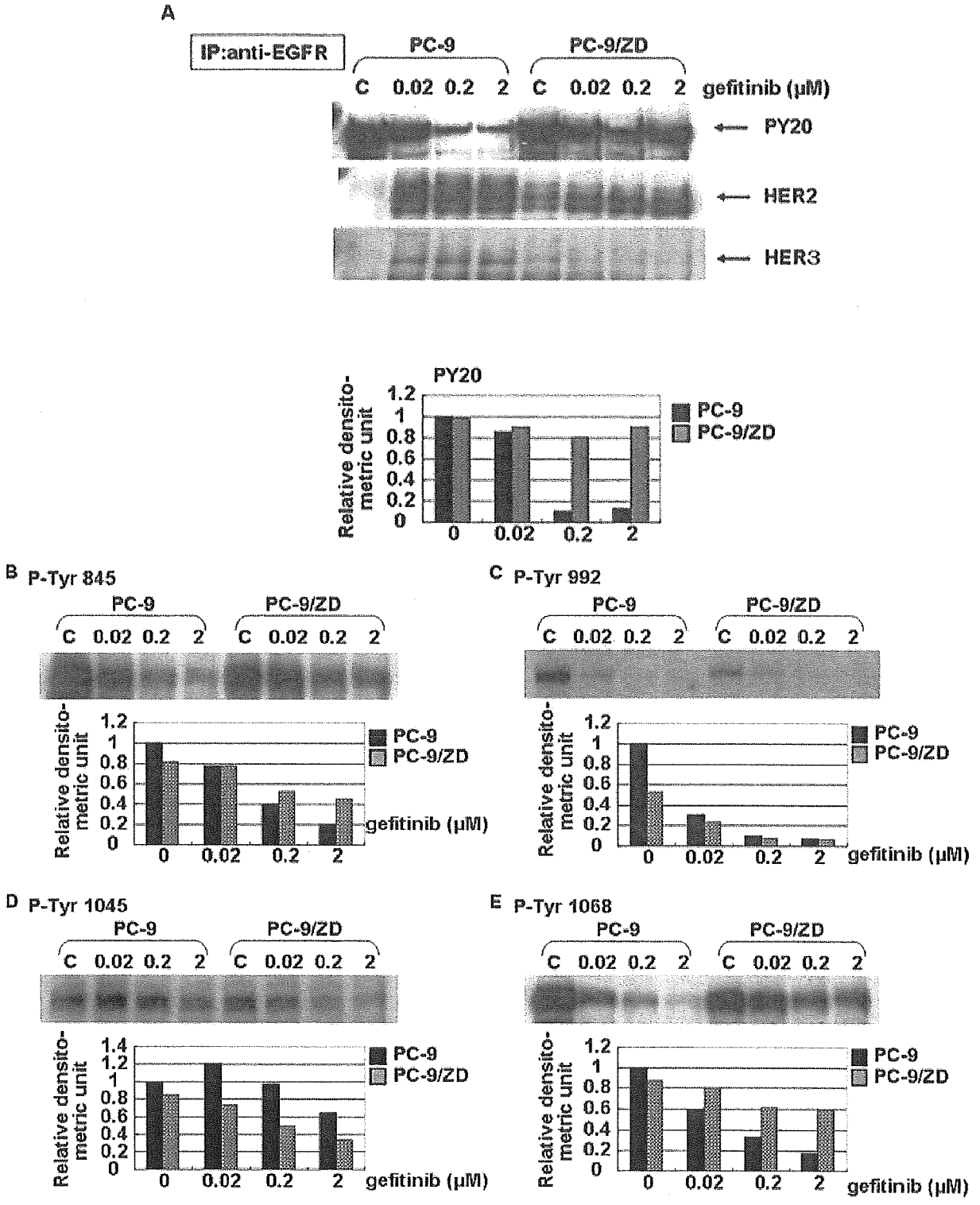

FIGURE 5 – Effect of gefitinib on autophosphorylation of EGFR. (*a*) PC-9 and PC-9/ZD cells (5×10^6) were exposed to 0.02, 0.2 or 2 μM gefitinib for 6 hr. The 1,500 μg of total cell lysate was immunoprecipitated with an anti-EGFR antibody. The immunoprecipitates were subjected to gel electrophoresis and Western blotting with anti-phosphotyrosine, anti-HER2 and anti-HER3 antibodies. Tyrosine-phosphorylated EGFR was determined with an anti-phosphotyrosine antibody. Heterodimer formation of EGFR was analyzed with anti-HER2 and anti-HER3 antibodies. The expression levels have been plotted in a graph. (*b–e*) PC-9 and PC-9/ZD cells were exposed to 0.02, 0.2 and 2 μM gefitinib for 6 hr. A 20 μg of protein of each sample was analyzed by Western blotting by using anti phospho-EGFR (Tyr845, Tyr992, Tyr 1045, Tyr 1068) antibodies.

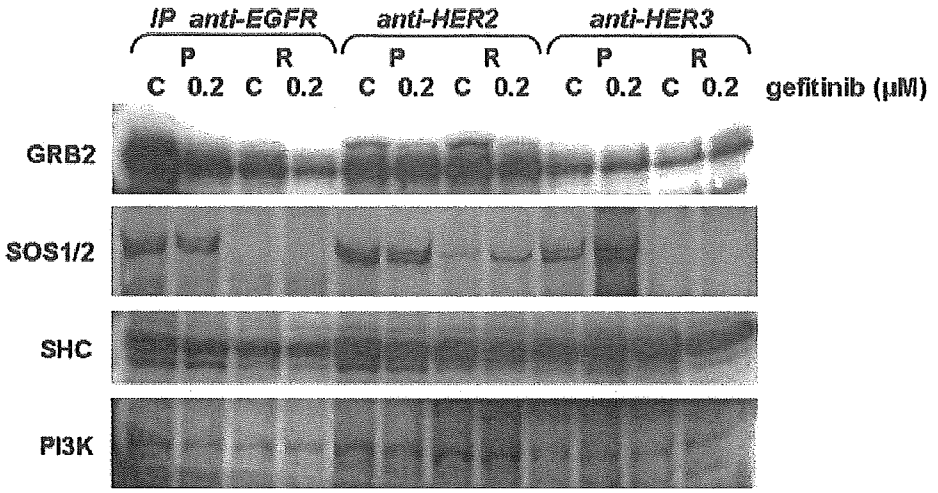

FIGURE 6 – Protein interaction between EGFR and its adaptor proteins. Cells (P: PC-9, R: PC-9/ZD) were exposed to 0 and 0.2 μM of gefitinib for 6 hr. The cells were lysed and immunoprecipitated with ant-EGFR, anti-HER2, and anti-HER3 antibodies, and the amounts of the Grb2, SOS1/2, SHC and PI3K precipitated were monitored by immunoblotting with their specific Abs.

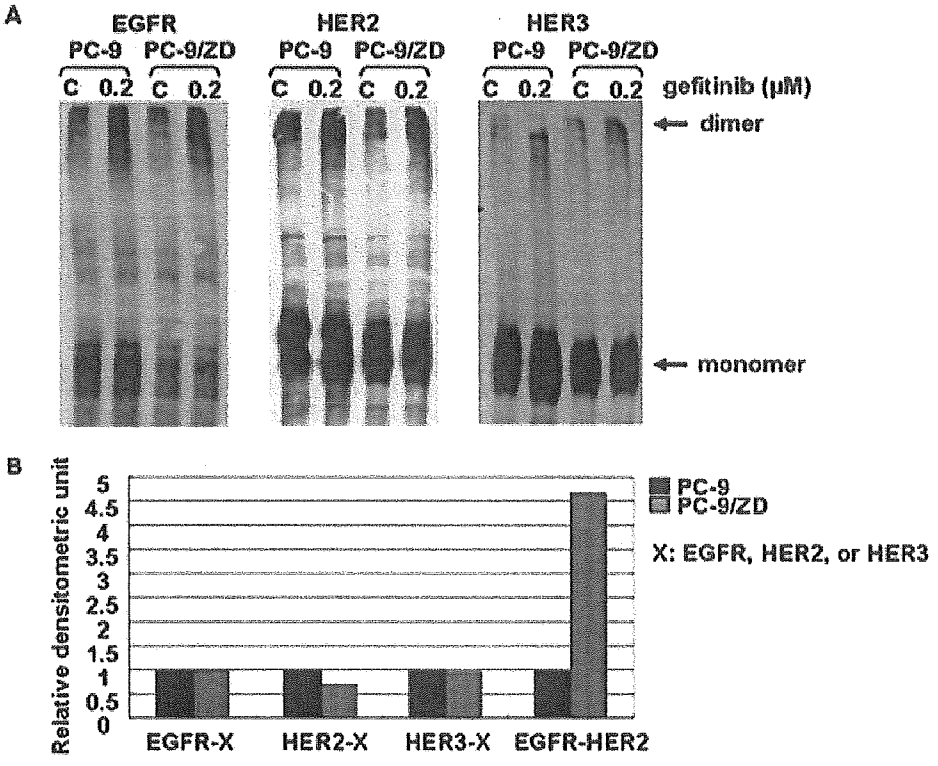

FIGURE 7 – Chemical cross-linking of PC-9 and PC-9/ZD cells. (*a*) After 6 hr exposure to 1.5 mM bis (sulfosuccinimidyl) substrate dissolved in PBS as indicated in Material and Methods. The cross-linking reaction was quenched and the cell lysates were prepared and subjected to immunoblot analysis of EGFR, HER2 and HER3. (*b*) Ratio of dimmers formed by PC-9 cells to those by PC-9/ZD cells in the absence of gefitinib. The density of the bands in (*a*) for EGFR-X, HER2-X and HER3-X were quantified densitometrically. The ratio of EGFR-HER2 was calculated by the band density obtained in Figure 5*a*. X = EGFR, HER2 or HER3.

Discussion

Interest in resistance to target-based therapy (TBT) has been growing ever since clinical efficacy was first demonstrated.[11–13] Although CML patients respond to STI-571 well at first, most patients eventually relapse in the late stage of the disease.[25–27] It has been reported that some patients in whom treatment with gefitinib is effective at first, ultimately become refractory.[30] Resistance is likely to remain a hurdle that limits the long-term effectiveness of TBT. PC-9 had a deletion mutation within the kinase domain of *EGFR* and is highly sensitive. These characters are similar to those of NSCLC with clinical responsiveness to gefitinib. Analyzing the mechanism of resistance of PC-9/ZD subline might be clinically meaningful.

The mechanism of drug resistance is thought to be multifactorial. Because the growth-inhibitory assay in our present study showed no cross resistance to a variety of cytotoxic agents, the mechanism of the resistance differs from the mechanism of multidrug resistance patterns. Although expression of BCRP, one of the multidrug-resistance-related proteins has been reported to contribute to the resistance to gefitinib,[31] expression of *BCRP* mRNA is observed only in PC-9 cells (data not shown). Although mutations in the ATP-binding pocket of *BCR-ABL* gene have been identified recently in cells from CML patients who were refractory to STI-571 treatment or relapse,[25–27] there have been no reports of any such mutations for gefitinib resistance. PC-9/ZD also became refractory to gefitinib without secondary mutation in *EGFR* cDNA. These suggest the possibility of refractory tumor after treatment of gefitinib including this kind of phenotype.

There is no significant difference in expression level of EGFR between PC-9 and PC-9/ZD. Does the antitumor effect of gefitinib

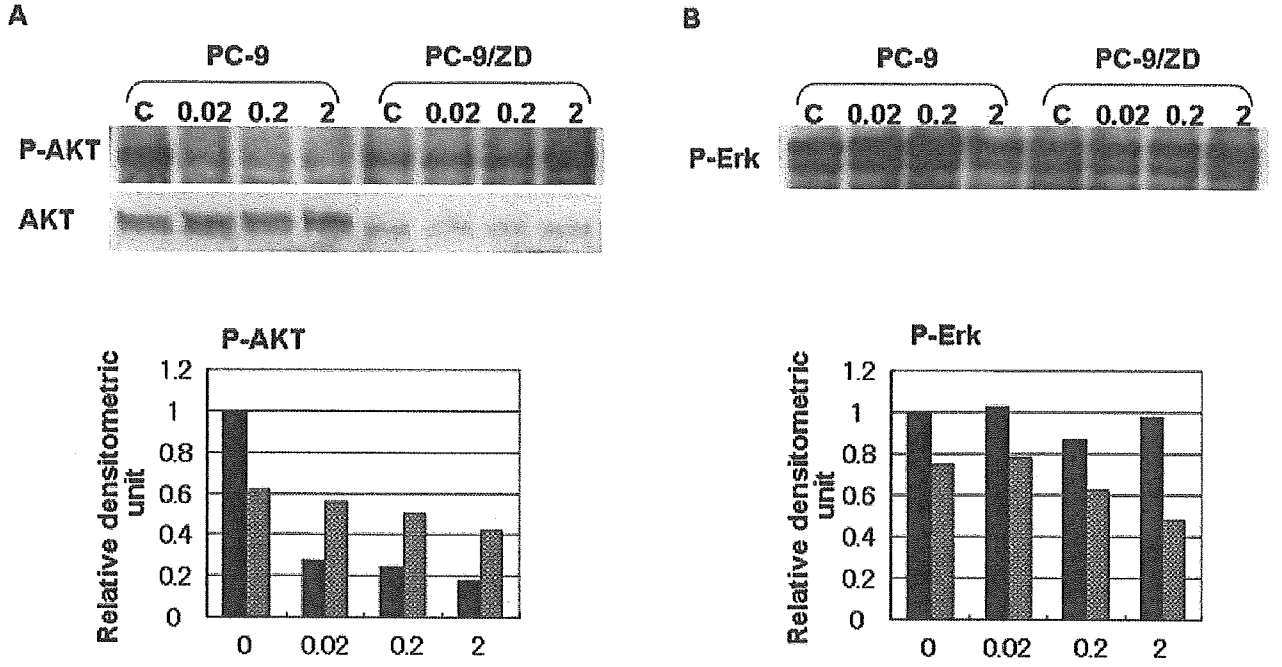

FIGURE 8 – Effect of gefitinib on the MAPK and AKT pathway. Cells were placed in medium containing 0, 0.02, 0.2 or 2 μM of gefitinib for 6 hr and harvested in EBC buffer. Total cellular lysates were separated on SDS-PAGE, transferred to a membrane and blotted with (*a*) anti-phospho-AKT (Ser473) and (*b*) anti-phospho-Erk (p44/42) antibodies. The expression levels are shown in a graph.

require EGFR expression? Naruse *et al.*[32] suggested that the high sensitivity of K562/TPA to gefitinib is due to acquired EGFR expression. In their study autophosphorylation of EGFR in K562/TPA cells was inhibited by 0.01 μM gefitinib, and the IC_{50}-value of gefitinib in parental K562 cells, which do not express EGFR, was approximately 400-fold higher than that in the K562/TPA subline. Furthermore, most patients who responded to gefitinib therapy have *EGFR* mutation in lung tumor.[18,19] These findings suggest strongly that gefitinib exerts its antitumor effect through an action on EGFR. Our present study showed similar EGFR expression and autophosphorylation levels in PC-9 and PC-9/ZD cells. The inhibitory effect of gefitinib on phosphorylation of EGFR is different. PC-9/ZD did not show cross-resistance to the specific EGFR TK inhibitors RG-14620 and Lavendustin A in an MTT assay, nor did inhibit the phosphorylation of EGFR at the cellular level (data not shown). Paez *et al.*[18] reported that phosphorylation of EGFR in gefitinib-resistant cell lines was inhibited only when gefitinib was present at high concentration. These findings suggest that the difference in the inhibitory-effect on EGFR phosphorylation may determine the efficacy of the drug.

The inhibitory effect of gefitinib on EGFR phosphorylation is not significant in PC-9/ZD cells despite the absence of differences in the sequences of *EGFR*, *HER2*, and *HER3*. There are several possible explanations for the difference in inhibitory effect. First, the avidity of gefitinib for the ATP-binding site of EGFR may be decreased in PC-9/ZD cells due to a protein-protein interaction, *i.e.*, EGFR and a certain protein prevent gefitinib from binding to EGFR. Second, a change in the activity of specific protein-tyrosine kinase or phosphatase of EGFR in PC-9/ZD cells, especially after exposure to gefitinib, may result in resistance to inhibition of EGFR phosphorylation. The phosphorylation level is maintained in exquisite balance by the reciprocal activities of kinase and phosphatase,[33,34] and Wu reported that phosphatase plays a role in STI571-resistance.[35] Third, increased heterodimer formation by EGFR with other members of the HER family results in the limited inhibition. Heterodimer formation is increased in PC-9/ZD cells under basal conditions, and no increase in formation was observed after exposure to gefitinib, although marked heterodimer induction was observed in PC-9 cells. Calculations in *in vitro* studies have shown that the IC_{50}-value for inhibition of the tyrosine kinase activity of EGFR is 0.023–0.079 μM, whereas the IC_{50}-value for inhibition of HER2 is 100-fold higher.[36] We estimate that the inhibitory effect of gefitinib depends on the ratio of homodimer formation to heterodimer formation, and the heterodimer may be one of the routes of escape from the action of gefitinib.

Signal transduction by the HER family member is mediated by 2 major pathways, the MAPK signaling pathway and the AKT signaling pathway, which regulate cell proliferation and survival. Because phosphorylated AKT was inhibited completely by gefitinib in PC-9 cells, but inhibition of phosphorylated MAPK was not significant, inhibition of the AKT pathway may be more important to cell sensitivity than inhibition of MAPK. Moasser *et al.*[37] reported consistent results, showing that downregulation of AKT activity is predominantly seen in tumors that are sensitive to gefitinib. The phosphorylation of AKT and MAPK was not inhibited significantly by gefitinib in PC-9/ZD cells. This finding might be attributable to inactivation of Tyr 1068-GRB2-SOS-mediated signaling.

Based on the results of this comparative study, EGFR-GRB2-SOS complex formation, phosphorylation of Tyr1068, the ratio of the amount of homodimer formation to heterodimer formation, and the AKT signaling pathway are possible predictive biomarkers for gefitinib sensitivity. As a different approach, we are now looking for the genes associated with gefitinib resistance in PC-9/ZD cells compared to PC-9 cells by subtractive cloning.

Acknowledgements

'Iressa' is a trademark of the AstraZeneca group of companies.

References

1. Socinski MA. Addressing the optimal duration of therapy in advanced, metastatic non-small-cell lung cancer. In: Perry MC, eds. American Society of Clinical Oncology Educational Book. Alexandria: Lisa Greaves, 2003;144–52.
2. Nicholson RI, Gee JM, Harper ME. EGFR and cancer prognosis. Eur J Cancer 2001;37:S9–15.
3. Mendelsohn J, Baselga J. The EGF receptor family as targets for cancer therapy. Oncogene 2000;19:6550–65.
4. Salmon DS, Brandt R, Ciardiello F, Normanno N. Epidermal growth factor-related peptides and their receptors in human malignancies. Crit Rev Oncol Hematol 1995;19:182–232.
5. Fox SB, Smith K, Hollyer J, Greenall M, Hastrich D, Harris AL. The epidermal growth factor receptor as a prognostic marker: result of 370 patients and review of 3009 patients. Breast Cancer Res Treat 1994;29:41–99.
6. Dassonville O, Formento JL, Francoual M, Ramaioli A, Santini J, Schneider M, Demard F. Expression of epidermal growth factor receptor and survival in upper aerodigestive tract cancer. J Clin Oncol 1993;11:1873–8.
7. Sainsbury JR, Farndon JR, Needham GK, Malcolm AJ, Harris AL. Epidermal-growth-factor receptor status as predictor of early recurrence of and death from breast cancer. Lancet 1987;1:1398–402.
8. Scambia G, Benedetti-Panici P, Ferrandina G, Distefano M, Salerno G, Romanini ME, Fagotti A, Mancuso S. Epidermal growth factor, oestrogen and progesterone receptor expression in primary ovarian cancer: correlation with clinical outcome and response to chemotherapy. Br J Cancer 1995;72:361–6.
9. Veale D, Ashcroft T, Marsh C, Gibson GJ, Harris AL. Epidermal growth factor receptors in non-small cell lung cancer. Br J Cancer 1987;55:513–6.
10. Veale D, Kerr N, Gibson GJ, Kelly PJ, Harris AL. The relationship of quantitative epidermal growth factor receptor expression in non-small cell lung cancer to long term survival. Br J Cancer 1993;68:162–5.
11. Druker BJ, Talpaz M, Resta DJ, Peng B, Buchdunger E, Ford JM, Lydon NB, Kantarjian H, Capdeville R, Ohno-Jones S, Sawyers CL. Efficacy and safety of a specific inhibitor of the BCR-ABL tyrosine kinase in chronic myeloid leukemia. N Engl J Med 2001;344: 1031–7.
12. Druker BJ, Sawyers CL, Kantarjian H, Resta DJ, Reese SF, Ford JM, Capdeville R, Talpaz M. Activity of a specific inhibitor of the BCR-ABL tyrosine kinase in the blast crisis of chronic myeloid leukemia and acute lymphoblastic leukemia with the Philadelphia chromosome. N Engl J Med 2001;344:1038–42.
13. Joensuu H, Roberts PJ, Sarlomo-Rikala M, Andersson LC, Tervahartiala P, Tuveson D, Silberman S, Capdeville R, Dimitrijevic S, Druker B, Demetri GD. Effect of the tyrosine kinase inhibitor STI571 in a patient with a metastatic gastrointestinal stromal tumor. N Engl J Med 2001;344:1052–6.
14. Fukuoka M, Yano S, Giaccone G, Tamura T, Nakagawa K, Douillard JY, Nishiwaki Y, Vansteenkiste J, Kudoh S, Rischin D, Eek R, Horai T, et al. Multi-institutional randomized phase II trial of gefitinib for previously treated patients with advanced non-small-cell lung cancer. J Clin Oncol 2003;21:2227–9.
15. Kris MG, Natale RB, Herbst RS, Lynch TJ Jr, Prager D, Belani CP, Schiller JH, Kelly K, Spiridonidis H, Sandler A, Albain KS, Cella D, et al. Efficacy of gefitinib, an inhibitor of the epidermal growth factor receptor tyrosine kinase, in symptomatic patients with non-small cell lung cancer: a randomized trial. JAMA 2003;290:2149–58.
16. Giaccone G, Herbst RS, Manegold C, Scagliotti G, Rosell R, Miller V, Natale RB, Schiller JH, Von Pawel J, Pluzanska A, Gatzemeier U, Grous J, *et al*. Gefitinib in combination with gemcitabine and cisplatin in advanced non-small-cell lung cancer: a phase III trial—INTACT 1. J Clin Oncol 2004;22: 777–84.
17. Miller VA, Johnson DH, Krug LM, Pizzo B, Tyson L, Perez W, Krozely P, Sandler A, Carbone D, Heelan RT, Kris MG, Smith R, et al. Pilot trial of the epidermal growth factor receptor tyrosine kinase inhibitor gefitinib plus carboplatin and paclitaxel in patients with stage IIIB or IV non-small-cell lung cancer. J Clin Oncol 2003;21: 2094–100.
18. Paez JG, Janne PA, Lee JC, Tracy S, Greulich H, Gabriel S, Herman P, Kaye FJ, Lindeman N, Boggon TJ, Naoki K, Sasaki H, et al. EGFR mutations in lung cancer: correlation with clinical response to gefitinib therapy. Science 2004;304:1497–500.
19. Lynch TJ, Bell DW, Sordella R, Gurubhagavatula S, Okimoto RA, Brannigan BW, Harris PL, Haserlat SM, Supko JG, Haluska FG, Louis DN, Christiani DC, et al. Activating mutations in the epidermal growth factor receptor underlying responsiveness of non-small-cell lung cancer to gefitinib. N Engl J Med 2004;350: 2191–3.
20. Pao W, Miller V, Zakowski M, Doherty J, Politi K, Sarkaria I, Singh B, Heelan R, Rusch V, Fulton L, Mardis E, Kupfer D, et al. EGF receptor gene mutations are common in lung cancers from "never smokers" and are associated with sensitivity of tumors to gefitinib and erlotinib. Proc Natl Acad Sci USA 2004; 101:13306–11.
21. Nomori H, Saijo N, Fujita J, Hyoi M, Sasaki Y, Shimizu E, Kanzawa F, Inomata M, Hoshi A. Detection of NK activity and antibody-dependent cellular cytotoxicity of lymphocytes by human tumor clonogenic assay—its correlation with the 51Cr-release assay. Int J Cancer 1985;35:449–55.
22. Mosmann T. Rapid colorimetric assay for cellular growth and survival: application to proliferation and cytotoxicity assays. J Immunol Meth 1983;65:55–63.
23. Arteaga CL, Ramsey TT, Shawver LK, Guyer CA. Unliganded epidermal growth factor receptor dimerization induced by direct interaction of quinazolines with ATP binding site. J Biol Chem 1998;273:18623–32.
24. Gorre ME, Mohammed M, Ellwood K, Hsu N, Paquette R, Rao PN, Sawyers CL. Clinical resistance to STI-571 cancer therapy caused by BCR-ABL gene mutation or amplification. Science 2001;293:876–80.
25. Von Bubnoff N. BCR-ABL gene mutation in relation to clinical resistance Lancet 2002;356:487–91.
26. McCormick F. New-age drug meets resistance. Nature 2001;412: 281–2.
27. Ricci C, Scappini B, Divoky V, Onida F, Verstovsek S, Kantarjian HM, Beran M. Mutation in the ATP binding pocket of the ABL kinase domain in and STI571-resistant BCR/ABL-positive cell line. Cancer Res 2002;62:5995–8.
28. Laffargue M, Raynal P, Yart A, Peres C, Wetzker R, Roche S, Payrastre B, Chap H. An epidermal growth factor receptor/Gab1 signaling pathway is required for activation of phosphoinositide 3-kinase by lysophosphatidic acid. J Biol Chem 1999;274:32835–41.
29. Rodriguez-Viciana P, Warne PH, Dhand R, Vanhaesebroeck B, Gout I, Fry MJ, Waterfield MD, Downward J. Phosphatidylinositol-3-OH kinase as a direct target of Ras. Nature 1994;370:527–32.
30. Kurata T, Tamura K, Kaneda H, Nogami T, Uejima H, Asai Go G, Nakagawa K, Fukuoka M. Effect of re-treatment with gefitinib ('Iressa', ZD1839) after acquisition of resistance. Ann Oncol 2004;15:173–4.
31. Yanase K, Tsukahara S, Asada S, Ishikawa E, Imai Y, Sugimoto Y. Gefitinib reverses breast cancer resistence protein-mediated drug resistence. Mol Cancer Ther 2004;3:1119–25.
32. Naruse I, Ohmori T, Ao Y, Fukumoto H, Kuroki T, Mori M, Saijo N, Nishio K. Antitumor activity of the selective epidermal growth factor receptor- tyrosine kinase inhibitor (EGFR-TKI) Iressatm (ZD1839) in a EGFR-expressing multidrug resistant cell line in vitro and in vivo. Int J Cancer 2002;98:310–5.
33. Reynolds AR, Tischer C, Verveer PJ, Rocks O, Bastiaens PIH. EGFR activation coupled to inhibition of tyrosine phosphatases causes lateral signal propagation. Nat Cell Biol 2003;5:447–53.
34. Haj FG, Markova B, Klaman LD, Bohmer FD, Neel BG. Regulation of receptor tyrosine kinase signaling by protein tyrosine phosphatase-1B. J Biol Chem 2003;278:739–44.
35. Wu JY, Talpaz M, Donato NJ. Tyrosine kinases and phosphatase play a role in STI571-mediate apoptosis of chronic myelogenous leukemia cells. Proc Am Assoc Cancer Res 2003;44(2nd ed.) 205:(Abstract 1016).
36. Wakeling AE, Guy SP, Woodburn JR, Ashton SE, Curry BJ, Barker AJ, Gibson KH. ZD1839 (Iressa): an orally active inhibitor of epidermal growth factor signaling with potential for cancer therapy. Cancer Res 2002;62:5749–54.
37. Moasser MM, Basso A, Averbuch SD, Rosen N. The tyrosine kinase inhibitor ZD1839 ("Iressa") inhibits HER2-driven signaling and suppresses the growth of HER2-overexpressing tumor cells. Cancer Res 2001;61:7184–8.

Eur Radiol
DOI 10.1007/s00330-005-0091-3

GASTROINTESTINAL

Ukihide Tateishi
Mototaka Miyake
Tetsuo Maeda
Yasuaki Arai
Kunihiko Seki
Tadashi Hasegawa

CT and MRI findings in KIT-weak or KIT-negative atypical gastrointestinal stromal tumors

Received: 25 July 2005
Revised: 28 September 2005
Accepted: 21 November 2005

U. Tateishi (✉) · M. Miyake · T. Maeda · Y. Arai
Division of Diagnostic Radiololgy and Nuclear Medicine,
National Cancer Center Hospital,
5-1-1, Tsukiji, Chuo-Ku,
104-0045, Tokyo, Japan
e-mail: utateish@ncc.go.jp
Tel.: +81-3-35422511
Fax: +81-3-35423815

K. Seki
Pathology Division,
National Cancer Center Hospital,
Tokyo, Japan

T. Hasegawa
Department of Clinical Pathology,
Sapporo Medical University
School of Medicine,
Sapporo, Japan

Abstract The large majority of gastrointestinal stromal tumors (GIST) can be diagnosed on the basis of KIT immunoreactivity. However, some atypical tumors show weak or negative KIT expression. We studied the imaging characteristics of atypical GIST, reviewing CT and MRI findings in ten patients (eight men, two women; mean age 59 years) with atypical GIST. Radiological studies were evaluated by two radiologists by consensus and included CT and MR imaging in all patients. Pathological diagnoses were made from surgery and confirmed by the polymerase-chain reaction (PCR) to amplify both exons of the c-kit gene and PDGFRA gene. The CT and MR examinations revealed a heterogeneous mass of the stomach containing cystic regions and soft tissue elements in all cases. All lesions were extraluminal masses and had an exophytic epicenter. On T1-weighted MR images soft tissue elements of the tumors were of homogeneously low- (n=3) or iso-signal intensity (n=7) compared with the liver parenchyma. On fast spin-echo T2-weighted MR images soft tissue elements of all tumors showed cystic regions of significantly high signal intensity interspersed with septumlike structures of low signal intensity. All lesions exhibited homogeneously (n=4) or heterogeneously (n=6) mild to moderate enhancement of soft tissue elements. Despite the relatively small number of patients CT and MRI findings of atypical GIST are a submucosal mass with soft tissue elements and cystic regions.

Keywords Gastrointestinal stromal tumor · Gastric tumor · Intestinal tumor · Stomach neoplasm

Introduction

Gastrointestinal stromal tumor (GIST) is a mesenchymal tumor of the gastrointestinal tract that accounts for 2.2% of all gastric tumors [1]. According to a specific molecular analysis most GISTs express consistent immunoreactivity for KIT, a c-kit proto-oncogene protein (CD 117 antigen) [2]. The result of immunohistochemical survey leads to distinguish between GISTs and other mesenchymal tumors arising from the gastrointestinal tract [3]. Most GISTs have oncogenic KIT mutations that are early events in the pathogenesis of GISTs and result in the proliferation of tumor cells. Because of this a Kit-selective tyrosine kinase inhibitor, imatinib mesylate (Gleevec, formerly known as STI571; Novartis, East Hanover, N.J., USA) has been found to have a significant efficacy as a chemotherapeutic agent [4, 5].

Computed tomography (CT) and magnetic resonance imaging (MRI) have become a well accepted method for diagnosis and staging of GISTs [6–10]. The CT and MRI findings suggest that conventional GISTs are well-defined extraluminal or intramural masses, whose CT attenuation and MR signal intensity depend on tumor size. The larger tumors frequently appear heterogeneous as a result of central necrosis, cystic change, hemorrhage, and homogeneous tumors have a shorter diameter [6–10]. Nonspecific imaging features, however, have also been reported in various neoplasms, and one cannot rule out that a

mesenchymal neoplasm other than a GIST in gastrointestinal tract constitutes a potential drawback for successful imaging of GIST [11].

Although the large majority of GISTs can be diagnosed on the basis of KIT immunoreactivity, some neoplasms show weak or negative KIT expression [12–14]. They usually involve the stomach and are very rare, accounting for less than 5% of all GISTs and approx. 10% of gastric GISTs [15, 16]. As concerns such rare tumors, the weak or negative KIT mutation affects accurate pathological diagnosis for GIST. A recent cytogenetic study revealed the existence of mutations of the platelet-derived growth factor receptor α (PDGFRA) gene which was also the product of the c-kit proto-oncogene in KIT-weak or KIT-negative GISTs [17].

To our knowledge, no series focusing on KIT-weak or KIT-negative GISTs has yet been reported in the radiology literature. We therefore reviewed the imaging characteristics of ten atypical GISTs whose diagnosis was confirmed by pathological and cytogenetic analyses. We particularly focused on comparing the imaging characteristics that we observed with those previously reported.

Materials and methods

A retrospective analysis of ten patients with KIT-weak or KIT-negative GISTs who underwent CT and MRI at our institution was performed (eight men, two women; mean age 59 years, range 43–73). Patients' medical database was reviewed for epidemiological, clinical and surgical findings. Nine patients presented with epigastric discomfort, nausea, vomiting or abdominal pain, and one mass was discovered when the patient was examined because of gastrointestinal bleeding at endoscopy. One had both abdominal pain and vomiting. All lesions arose in the stomach. Seven lesions were located in the body of the stomach, two in the antrum, and one in the cardia. Our institutional review board does not require its approval or patient informed consent for this type of review.

Radiological studies of each lesion were evaluated by two radiologists by consensus and included CT with and without contrast enhancement in all patients, and MR imaging with high-field (1.5-T) units in all patients. The CT examinations were performed with the patient in the supine position, and patients were also injected with iodinated nonionic contrast material (300 mg/ml iodine) intravenously at a rate of 3.0 ml/s for a total of 100 ml with an autoinjector. Patients were also given water of 300 ml as oral contrast. The scanning parameters of CT were: axial 4- or 16- slice mode, 1.0–5.0 mm section thickness, 0.5 s rotation, 120–150 kVp, 200–250 mA. Section thickness ranged between 5 and 10 mm by reconstruction using a standard algorithm.

T1- and T2-weighted MR images were obtained in the transverse plane and at least one longitudinal plane with a body coil. T1-weighted spin echo (SE) or fast spin-echo (FSE) acquisitions were obtained by using a 24–30 cm field of view, 4–8 mm section thickness, 400–620/8.9–15 (repetition time ms/echo time ms), 256×192–224 matrix, two signals acquired. T2-weighted FSE acquisitions were performed using a 24–35 cm field of view, 4–8 mm section thickness, 3,000–12,000/80–120 (repetition time ms/echo time ms), 256×192–224 matrix, and two signals were acquired. After the intravenous administration of 0.1 mmol gadopentate dimeglumine (Magnevist, Schering, Berlin, Germany) per kilogram body weight, transverse T1-weighted MR images with fat suppression were obtained in the transverse plane and at least one longitudinal plane.

Two board-certified radiologists retrospectively reviewed the CT and MR images, and their findings were reported as a consensus opinion. Images were evaluated for lesion location and size, shape of the interface (regular or irregular), endoluminal or extraluminal mass, epicenter (intrinsic or exophytic), cystic region, soft tissue elements, hemorrhage, intratumoral and capsular calcification, ulceration, central gas, fistula, infiltration of other organ, peritoneal dissemination, hepatic metastasis, enlargement of lymph node, ascites, and distant metastasis. MR images were evaluated for predominant signal intensity characteristics (low, intermediate, or high), signal homogeneity or heterogeneity, as well as enhancement characteristics. On T1-weighted MR images low signal intensity was defined as signal intensity less than that of muscle, intermediate signal intensity as similar to that of muscle, and high signal intensity as similar to that of fat. On FSE T2-weighted MR images low signal intensity was defined as signal intensity similar to that of muscle, intermediate signal intensity as greater than that of muscle, but less than that of fat, and high signal intensity as equal to or greater than that of fat. Tumor enhancement was visually graded as greater than, less than, or equal to that of surrounding muscle and vessels.

The cut surface, internal characteristics, and microscopic findings of the lesions were compared with the CT and MRI findings. Correlations between the imaging and histological findings were made by consensus between the radiologists and pathologists. Formalin-fixed and paraffin-embedded specimens were used for the histopathological and immunohistochemical studies and for the analyses for c-kit and PDGFRA gene mutations. A polyclonal antibody was used for KIT (DakoCytomation, Glostrup, Denmark, 1:50) [18]. Genomic DNA was extracted from formalin-fixed, paraffin-embedded specimens and amplified by the polymerase-chain reaction (PCR) to amplify exons 9, 11, 13, and 17 of the c-kit gene and exons 12 and 18 of the PDGFRA gene [15, 16]. We distinguished GISTs from leiomyosarcomas based on the immunoreactivity for KIT, desmin (DakoCytomation, 1:100), smooth-muscle actin (SMA; DakoCytomation, 1:100), and h-caldesmon (HCD; DakoCytomation, 1:100) [19].

Follow-up information was available in all cases. Follow-up contrast-enhanced CT examinations were per-

formed every 3–6 months after surgery. In one patient who was administered imatinib mesylate, follow-up contrast-enhanced CT was performed every month. Deaths confirmed to be caused by their disease were treated as an endpoint, and deaths from other causes were treated as censored observations. The disease-free date was recorded as the date when the medical record documented absence of any evidence of disease.

Results

Imaging findings

All lesions available for review on CT and MR examinations were detected (Table 1). Eight tumors had an irregular interface, and the other two had a regular interface. All lesions were extraluminal masses and had an exophytic epicenter. The average size of the tumors measured in the greatest dimension was 74 mm (range, 35–190 mm). The CT and MR examinations revealed a heterogeneous mass containing cystic regions and soft tissue elements in all cases (Figs. 1, 2, 3, 4). Unenhanced CT images of all lesions showed heterogeneous iso- (n=7) or hypo-attenuation (n=3) relative to the liver. None of the tumors had intratumoral or capsular calcification on unenhanced CT images. Soft tissue elements of the tumors were homogeneously (n=6) or heterogeneously (n=4) enhanced on contrast-enhanced CT images (Fig. 1). The attenuation of soft tissue elements was less than that of the aorta but greater than that of the liver parenchyma (n=7). Three tumors had soft tissue elements that were iso-attenuated relative to liver parenchyma on contrast-enhanced CT. In one tumor of the antrum the proportion of soft tissue element in the tumor predominated. Ulceration with detectable central gas was detected on CT in one lesion (Fig. 2). One patient had multifocal lesions and peritoneal dissemination (Fig. 3). Involvement of the gastrohepatic ligament was seen in three cases and involvement of the gastrosplenic ligament in two cases. On T1-weighted MR images soft tissue elements of the tumors were homogeneously low- (n=3) or iso-signal intensity (n=7) compared with the liver parenchyma. One lesion showed focal areas of high signal intensity, likely hemorrhagic regions. On FSE T2-weighted MR images soft tissue elements of all tumors showed predominantly increased T2 signal intensity relative to the liver parenchyma, and the images showed cystic regions of significantly high signal intensity interspersed with septumlike structures of low signal intensity (Figs. 2 and 4). All lesions exhibited homogeneously (n=4) or heterogeneously (n=6) mild to moderate enhancement of soft tissue elements and lack of obvious enhancement of cystic regions on contrast-enhanced MR images (Fig. 2). None of the CT or MRI images showed evidence of gastric fistula, liquefactive necrosis, infiltration of other organs, lymph node enlargement, or hepatic metastasis.

Table 1 CT and MRI findings of atypical GIST

	n
Primary tumor	10
Interface	
Regular	2
Irregular	8
Extraluminal mass	10
Exophytic epicenter	10
Cystic region and soft tissue elements	10
Unenhanced CT attenuation	
Iso	7
Hypo	3
Enhancement pattern[a]	
Homogeneous	6
Heterogeneous	4
Enhancement degree*	
Hyper	7
Iso	3
MR signal intensity[a]	
T1-weighted image	Low 3, iso 7
T2-weighted image	High 10
Septumlike structure[b]	10
Secondary tumor	3
Peritoneal dissemination	3
Cystic region and soft tissue elements	3

[a]Note. Imaging findings of soft tissue elements are presented
[b]Septumlike structure was depicted on T2-weighted image

Pathological findings

The gross and microscopic characteristics of the resected specimens corresponded to the CT and MRI findings. All tumors were characterized macroscopically by soft tissue masses with cystic regions (Figs. 1 and 4). Myxoid degeneration was present in the cystic regions of seven lesions. One lesion had an irregular margin and exhibited central ulceration. Necrosis (n=3) and hemorrhage (n=1) were identified in the samples of four tumors. Histological examination revealed epithelioid cells presenting eosinophilic cytoplasm and peripherally placed nuclei with myxoid stroma in nine tumors (Fig. 1). In one case the tumor consisted of spindle and epithelioid cells in varying ratios. Three tumors were of high risk, two were of intermediate risk, and five were of low risk. Eight tumors showed weakly positive immunostaining for KIT and the other two tumors were completely negative. None of the tumors had a c-kit gene mutation. On the other hand, PDGFRA gene mutations were identified in all cases.

All patients but one underwent surgical resection as a primary therapy. The surgical margins were adequate in eight

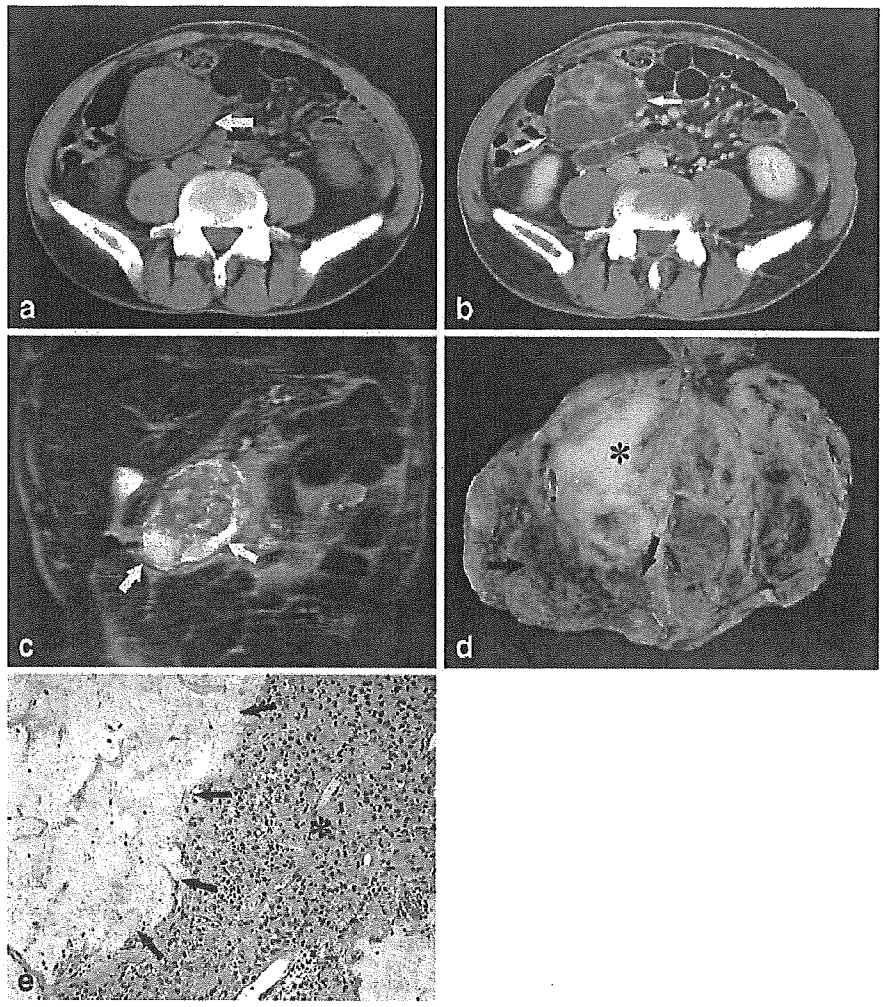

Fig. 1 A 69-year-old man with epigastric discomfort. **a** Unenhanced CT shows heterogeneous antral mass (*arrow*). **b** Contrast-enhanced CT reveals a mass in antrum with heterogeneous enhancement (*arrow*). **c** Coronal T2-weighted fast spin echo MRI (TR/TE_{eff}, 12,000 ms/80 ms) shows a cystic components with significantly high signal intensity (*arrows*). **d** Photograph of the gross specimen shows cystic components (*arrows*) and soft tissue elements (*asterisk*) in an antral mass. **e** Photomicrograph of the tumor shows oval epithelioid cells containing eosinophilic cytoplasm and peripherally placed nuclei (asterisk) with an abundant myxoid background (*arrows*). Hematoxylin and eosin stain; original magnification ×100

cases and inadequate in one case. In the patient with inadequate surgical margins wide resection was performed subsequently. One patient who developed peritoneal dissemination received oral imatinib mesylate therapy (400 mg per day) because the pathological examination of the resected specimens revealed weak-positive immunostaining for KIT.

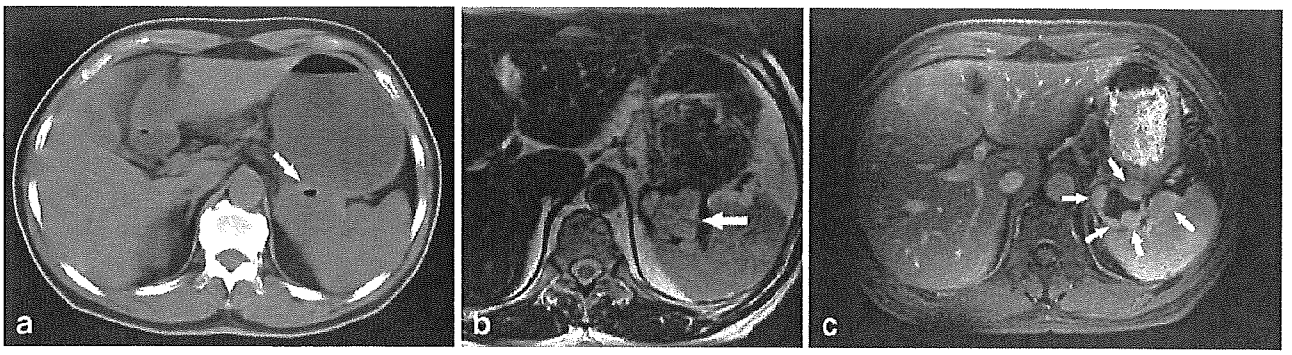

Fig. 2 A 72-year-old man with abdominal pain. **a** Unenhanced CT shows a heterogeneous mass in the gastric body that contains central gas (*arrow*). **b** Transverse T2-weghted fast spin echo MRI (2550/120) shows central cystic regions of high signal intensity interspersed with septumlike structures of low signal intensity (*arrow*). **c** Transverse fat saturated contrast-enhanced T1-weighted SE MRI (400/8.9) shows heterogeneously mild to moderate enhancement of soft tissue elements (*arrows*) and lack of obvious enhancement of the cystic region

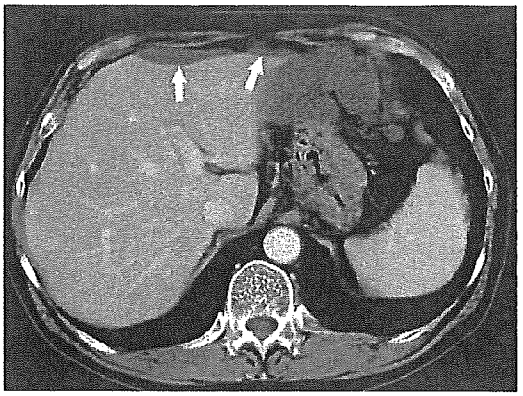

Fig. 3 A 52-year-old man with abdominal pain. Contrast-enhanced CT scan shows masses with significantly decreased density in the gastric body and hepatic surface consistent with peritoneal dissemination (*arrows*)

In this patient mild remission was observed for 16 months, but tumor regrowth was identified 18 months after the initial administration of imatinib mesylate. Tumor showed enlarged cystic mass and soft tissue elements with pronounced enhancement on CT. The median follow-up period of all cases was 65 months. Two other patients developed peritoneal dissemination after initial resection, but did not received imatinib mesylate because the pathological examination showed negative immunostaining for KIT. Recurrent tumors of these two patients also showed cystic mass and soft tissue elements with enhancement on CT. None of the cases developed visceral metastases. One patient with peritoneal disemination has died of the disease, and nine patients are alive with disease and seven with no evidence of disease.

Discussion

GISTs are generally characterized by genetic mutations of c-kit and highly sensitive to immunostaining of KIT which can be distinguished from other mesenchymal tumors of gastrointestinal tract. Recent advances in molecular targeting therapy reveals that imatinib mesylate (Gleevec, formerly known as STI571), which is a KIT-selective tyrosine kinase inhibitor, has a significant efficacy against metastatic or unresectable lesions in patients with KIT-positive GISTs [4, 5]. On the other hand, recent pathological studies have shown that the existence of KIT-weak or KIT-negative GISTs [12–16]. While making a correct pathological diagnosis is not usually a problem in patients with KIT-positive GISTs, it might be more difficult to establish a definite diagnosis in patients with KIT-weak or KIT-negative tumors.

Most atypical GISTs occur in the stomach, omentum, or mesentery [12–16]. Tumors arising from the duodenum and small intestine are less frequent than conventional GISTs. In our study seven tumors were extraluminal masses arising from the gastric body. The gastrohepatic ligament or gastrosplenic ligament was involved in many of them.

The imaging features of atypical GISTs reflect the underlying pathological findings. CT and MRI findings included a large extraluminal mass with heterogeneous lesion containing cystic regions and soft tissue elements. Cross-sectional imaging clearly depicted the gastric origin, extraluminal epicenter, and intrinsic characteristics of the tumors, and they corresponded to the pathological composition of the lesion. CT and MR images demonstrated cystic regions in all tumors of our series, with various degrees of soft tissue elements. Conventional GISTs appear an ill-defined mass with extrinsic or extraluminal epicenter, and internal areas of hemorrhage, necrosis, and cystic change are frequent causes of density or signal changes on CT and MRI [6–10]. Sandrasegaran and colleagues [6] reported that central hypoattenuation due to necrosis or apoptosis was identified in 33% of conventional gastric GISTs. Larger tumors may undergo massive liquefactive necrosis and cystic change leaving a rim of viable tissue.

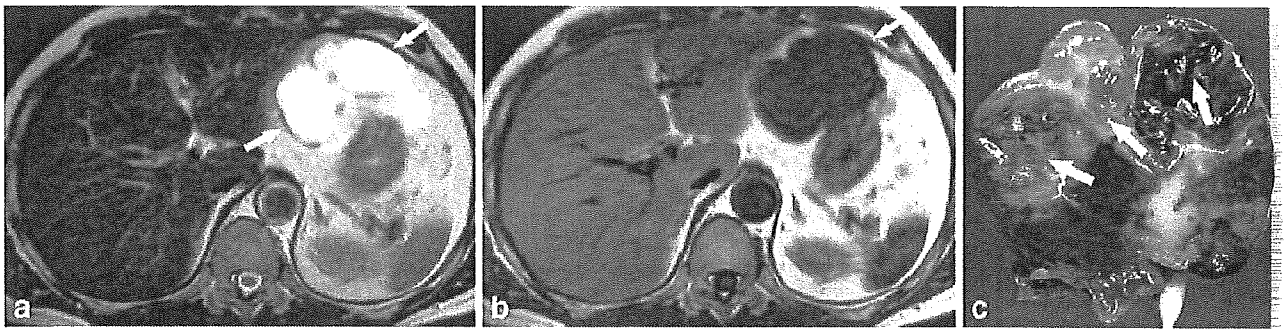

Fig. 4 A 60-year-old man with nausea and vomiting. **a** Transverse T2-weighted fast spin echo MRI (4000/112) shows a predominantly cystic mass (*arrows*) in the body of stomach with no evidence of infiltration. **b** Transverse T1-weighted SE MR image (550/15) shows soft tissue elements with homogeneously low signal intensity (*arrow*). **c** Photograph of gross pathology specimen shows cystic regions (*arrows*)

Therefore it is impossible to diagnose atypical GISTs from conventional GISTs based on CT and MRI findings. Imaging features of cystic regions and soft tissue elements are not specific but characteristic in atypical GISTs.

Myxoid degeneration or cystic change in tumors can occur after the treatment with imatinib mesylate which is one of the molecular-targeted chemotherapeutic agent and tyrosine kinase inhibitor [21–23]. Active metabolites of imatinib mesylate block the adenosine triphosphate binding site of tyrosine kinase. Morphological response to imatinib mesylate therapy has been reported in a tendency toward liquefaction before the tumor diminishes in size [21]. Choi and colleagues [22] described that the mean tumor density on CT decreased significantly after 2 months of treatment with imatinib mesylate compared with baseline. Pathological examination revealed a significant reduction in number of tumor cells and a hypocellular myxohyaline stroma. Myxoid or cystic change after treatment of imatinib mesylate often accompanied by a rim of soft tissue attenuation elements on CT and MRI. It is usually not possible to radiologically distinguish atypical GISTs from myxoid or cystic tumors treated by imatinib mesylate.

It may be important to make the distinction of atypical GIST from conventional GIST because of the difference in clinical behavior and patient prognosis. Sakurai and colleagues [16] reported 30 patients with atypical GISTs and 24 alive patients with mean follow-up period of 62 months. In our study only one patient died in a long period of follow-up and nondeveloped distant metastases except peritoneal dissemination. This evidence suggests that atypical GISTs have better prognosis than conventional GISTs. A recent study has revealed that imatinib mesylate can also bind and inhibit PDGFRA similar to KIT [14]. However, response to this drug in atypical GISTs is unclear and further clinical trials are needed.

Since KIT-weak and KIT-negative GISTs are rare, the number of cases in our retrospective study was rather small. While our limited data do not allow precise conclusions as to whether CT and MRI findings are helpful in diagnosing KIT-weak or KIT-negative GISTs, they do suggest that patients with a gastric submucosal tumor containing cystic regions and soft tissue elements should be cytogenetically tested for a PDGFRA mutation even if immunohistochemical survey shows that the lesion is weak or negative for KIT. More prospective studies are needed to define the value of CT and MRI as diagnostic tools in patients with an atypical GIST.

In conclusion, our review of data from ten patients with confirmed atypical GIST revealed characteristic findings. Tumors have the appearance of a submucosal tumor containing cystic regions and soft tissue elements on CT and MRI. These tumors are considered to be a variant of GIST which may represent mutation of KIT but PDGFRA by cytogenetic analysis.

Acknowledgements This work was supported in part by grants for Scientific Research Expenses for Health and Welfare Programs, No. 17-12 and BMS Freedom to Discovery Grant.

References

1. Miettinen M, Lasota J (2001) Gastrointestinal stromal tumors—definition, clinical, histological, immunohistochemical and molecular genetic features and differential diagnosis. Virchows Arch 438:1–12
2. Rossi C, Mocellin S, Mencarelli R et al (2003) Gastrointestinal stromal tumors: from a surgical to a molecular approach. Int J Cancer 107:171–176
3. Nishida T, Hirota S (2001) Biological and clinical review of stromal tumors in the gastrointestinal tract. Histol Histopathol 15:1293–1301
4. Singer S, Rubin BP, Lux ML et al (2002) Prognostic value of KIT mutation type, mitotic activity, and histologic subtype in gastrointestinal stromal tumors. J Clin Oncol 20:3898–3905
5. Heinrich MC, Corless CL, Demetri GD et al (2003) Kinase mutations and imatinib response in patients with metastaticgastrointestinal stromal tumor. J Clin Oncol 21:4342–4349
6. Sandrasegaran K, Rajesh A, Rushing DA et al (2005) Gastrointenstinal stromal tumors: CT and MRI findings. Eur Radiol 15:1407–1414
7. Ghanem N, Altehoefer C, Furtwangler A et al (2003) Computed tomography in gastrointestinal stromal tumors. Eur Radiol 13:1669–1678
8. Horton KM, Juluru K, Montogomery E et al (2004) Computed tomography imaging of gastrointestinal stromal tumors with pathology correlation. J Comput Assist Tomogr 28:811–817
9. Kim HC, Lee JM, Kim SH et al (2005) Small gastrointestinal stromal tumours with focal areas of low attenuation on CT: pathological correlation. Clin Radiol 60:384–388
10. Takao H, Yamahira K, Doi I et al (2004) Gastrointestinal stromal tumor of the retroperitoneum: CT and MR findings. Eur Radiol 14:1926–1929
11. Buckley JA, Fishman EK (1998) CT evaluation of small bowel neoplasms: spectrum of disease. Radiographics 18:379–392
12. Subramanian S, West RB, Corless CL et al (2004) Gastrointestinal stromal tumors (GISTs) with KIT and PDGFRA mutations have distinct gene expression profiles. Oncogene 23:7780–7790
13. Debiec-Rychter M, Wasag B, Stul M et al (2004) Gastrointestinal stromal tumours (GISTs) negative for KIT (CD117 antigen) immunoreactivity. J Pathol 202:430–438
14. Medeiros F, Corless CL, Duensing A et al (2004) KIT-negative gastrointestinal stromal tumors: proof of concept and therapeutic implications. Am J Surg Pathol 28:889–894
15. Wasag B, Debiec-Rychter M, Pauwels P et al (2004) Differential expression of KIT/PDGFRA mutant isoforms in epithelioid and mixed variants of gastrointestinal stromal tumors depends predominantly on the tumor site. Mod Pathol 17:889–894

16. Sakurai S, Hasegawa T, Sakuma Y et al (2004) Myxoid epithelioid gastrointestinal stromal tumor (GIST) with mast cell infiltrations: a subtype of GIST with mutations of platelet-derived growth factor receptor alpha gene. Hum Pathol 35:1223–1230
17. Hirota S, Ohashi A, Nishida T et al (2003) Gain-of-function mutations of platelet-derived growth factor receptor alpha gene in gastrointestinal stromal tumors. Gastroenterology 125:660–667
18. Hasegawa T, Matsuno Y, Shimoda T et al (2002) Gastrointestinal stromal tumor: consistent CD117 immunostaining for diagnosis, and prognostic classification based on tumor size and MIB-1 grade. Hum Pathol 33:669–676
19. Yamaguchi U, Hasegawa T, Matsuda T et al (2004) Differential diagnosis of gastrointestinal stromal tumor and other spindle cell tumors in the gastrointestinal tract based on immunohistochemical analysis. Virchows Arch 445:142–150
20. Trupiano JKR, Stewart RE, Misick C et al (2002) Gastric stromal tumors: a clinicopathologic study of 77 cases with correlation of features with nonaggressive and aggressive clinical behaviors. Am J Surg Pathol 26:705–714
21. Antoch G, Kanja J, Bauer S et al (2004) Comparison of PET, CT, and dual-modality PET/CT imaging for monitoring of imatinib (STI571) therapy in patients with gastrointestinal stromal tumors. J Nucl Med 45:357–365
22. Choi H, Charnsangavej C, de Castro Faria S et al (2004) CT evaluation of the response of gastrointestinal stromal tumors after imatinib mesylate treatment: a quantitative analysis correlated with FDG PET findings. AJR Am J Roentgenol 183:1619–1628
23. Busalacchi PJ Sr, de la Calle MA, Torroba A et al (2005) Gastrointestinal stromal tumor with metastases in an adult woman treated with imatinib mesylate: MDCT findings. AJR Am J Roentgenol 184:S58–S61